Geometry and valley-fill stratigraphic framework for aquifers in the Groundbirch paleovalley assessed through shallow seismic and ground-based electromagnetic surveys

Adrian S. Hickin, Melvyn E. Best, and André Pugin

BRITISH COLUMBIA
Ministry of Energy and Mines

BRITISH COLUMBIA GEOLOGICAL SURVEY

Ministry of Energy and Mines, British Columbia Geological Survey
Open File 2016-5

BRITISH COLUMBIA | Ministry of Energy and Mines

Geometry and valley-fill stratigraphic framework for aquifers in the Groundbirch paleovalley assessed through shallow seismic and ground-based electromagnetic surveys

Adrian S. Hickin
Melvyn E. Best
André Pugin

Ministry of Energy and Mines
British Columbia Geological Survey
Open File 2016-5

Ministry of Energy and Mines
Mines and Mineral Resources Division
British Columbia Geological Survey

Recommended citation: Hickin, A.S., Best, M.E., and Pugin, A., 2016. Geometry and valley-fill stratigraphic framework for aquifers in the Groundbirch paleovalley assessed through shallow seismic and ground-based electromagnetic surveys. British Columbia Ministry of Energy and Mines, British Columbia Geological Survey Open File 2016-5, 46p.

Front cover: Quaternary paleovalley fill sediments overlying shale at section 6 (Serpents Head) on the Murray River (Fig. 3). The succession at this location includes pre-late Wisconsinan glacial diamict overlain by late Wisconsinan advance phase glaciolacustrine silt and sand (glacial Lake Mathews; Unit 7), advance phase alluvial sand, gravel and diamict (Unit 8), diamicts of the late Wisconsinan glacial complex (Unit 9), and retreat phase glaciolacustrine silt, sand, clay and diamict (glacial Lake Peace; Unit 10).

Back cover: Geological Survey of Canada's minivib seismic vibrator with mobile geophone landstreamer collecting seismic data along the Stucky Road in the Groundbirch area of northeast British Columbia.

All British Columbia Geological Survey publications are available, free of charge, from:
http://www.empr.gov.bc.ca/Mining/Geoscience/PublicationsCatalogue/Pages/default.aspx

Appendices for this paper can be downloaded from
http://www.empr.gov.bc.ca/Mining/Geoscience/PublicationsCatalogue/OpenFiles/2016/Pages/2016-5.aspx

Geometry and valley-fill stratigraphic framework for aquifers in the Groundbirch paleovalley assessed through shallow seismic and ground-based electromagnetic surveys

Adrian S. Hickin[1a], Melvyn E. Best[2], and André Pugin[3]

[1]British Columbia Geological Survey, Ministry of Energy and Mines, Victoria, B.C., V8W 9N3
[2]Bemex Consulting International, 3701 Wild Berry Bend, Victoria, B.C., V9C 4M7
[3]Geological Survey of Canada, Natural Resources Canada, Ottawa, ON, K1A 0E8
[a]corresponding author: Adrian.Hickin@gov.bc.ca

Recommended citation: Hickin, A.S., Best, M.E., and Pugin, A., 2016. Geometry and valley-fill stratigraphic framework for aquifers in the Groundbirch paleovalley assessed through shallow seismic and ground-based electromagnetic surveys. British Columbia Ministry of Energy and Mines, British Columbia Geological Survey Open File 2016-5, 46p.

Abstract
Paleovalleys are significant sources of groundwater in the South Peace River region. To better understand groundwater availability it is necessary to determine the thickness, lateral extent, and connectivity of Quaternary sediments filling these paleovalleys. Direct observations of subsurface lithologic units (through sediment coring) combined with ground-based electromagnetic (EM) and shallow reflection seismic surveys document the geometry of the Groundbirch paleovalley and establish the three-dimensional configuration of its sediment fill. The combined data suggest that the Groundbirch paleovalley is 3-4 km wide at its top and trends east-west. Based mainly on seismic velocity data, the paleovalley may plunge to the west. Although the EM and seismic data are only effective in the upper 150 m, our interpretation of the seismic data suggests that the paleovalley may extend to depths of >350 m, an interpretation that can be tested by drilling. The stratigraphy of the valley fill includes advance phase glaciolacustrine sediments (glacial Lake Mathews), ice-contact glacial sediments (Late Wisconsinan glaciation), and retreat phase glaciolacustrine sediments (glacial Lake Peace). Gravels and sands deposited during ice margin advance and retreat have the highest potential to host significant aquifers.

Supplementary materials: All appendices can be downloaded from the British Columbia Geological Survey website at http://www.empr.gov.bc.ca/Mining/Geoscience/PublicationsCatalogue/OpenFiles/2016/Pages/2016-5.aspx

Keywords: Peace River, Groundbirch paleovalley, aquifer, groundwater, Quaternary, glacial stratigraphy, seismic velocity data, EM data, Late Wisconsinan glaciation, glacial Lake Matthews, glacial Lake Peace

1. Introduction

In northeastern British Columbia, water supports domestic, agricultural and industrial activities. However, as populations grow and industry expands, pressure on water supplies increases. Hence a better understanding of water systems and availability is needed to develop management practices that ensure equitable and sustainable use and continued economic development. In 2012 a collaborative study (Northeast British Columbia Aquifer Project) was established to evaluate the regional hydrogeology in northeast British Columbia and to characterize groundwater aquifers in the South Peace region (Wilford et al., 2012). This project included the BC Ministry of Forests, Lands and Natural Resource Operations, Ministry of Environment, Ministry of Energy and Mines, BC Oil and Gas Commission, Simon Fraser University, Geoscience BC, and the Geological Survey of Canada. The present study is part of this larger project and focuses on an area 40 km west of Dawson Creek (Fig. 1).

Paleovalleys are of particular interest in the South Peace River region because they are significant sources of groundwater and typically have higher yields than other potential aquifers (Cowen 1998). Buried paleovalleys host significant accumulations of heterogeneous sediment. Depending on stratigraphic and hydrogeologic constraints, coarse-grained units in paleovalley fills may host both confined and unconfined aquifers. Determining the thickness, lateral extent, and connectivity of such units

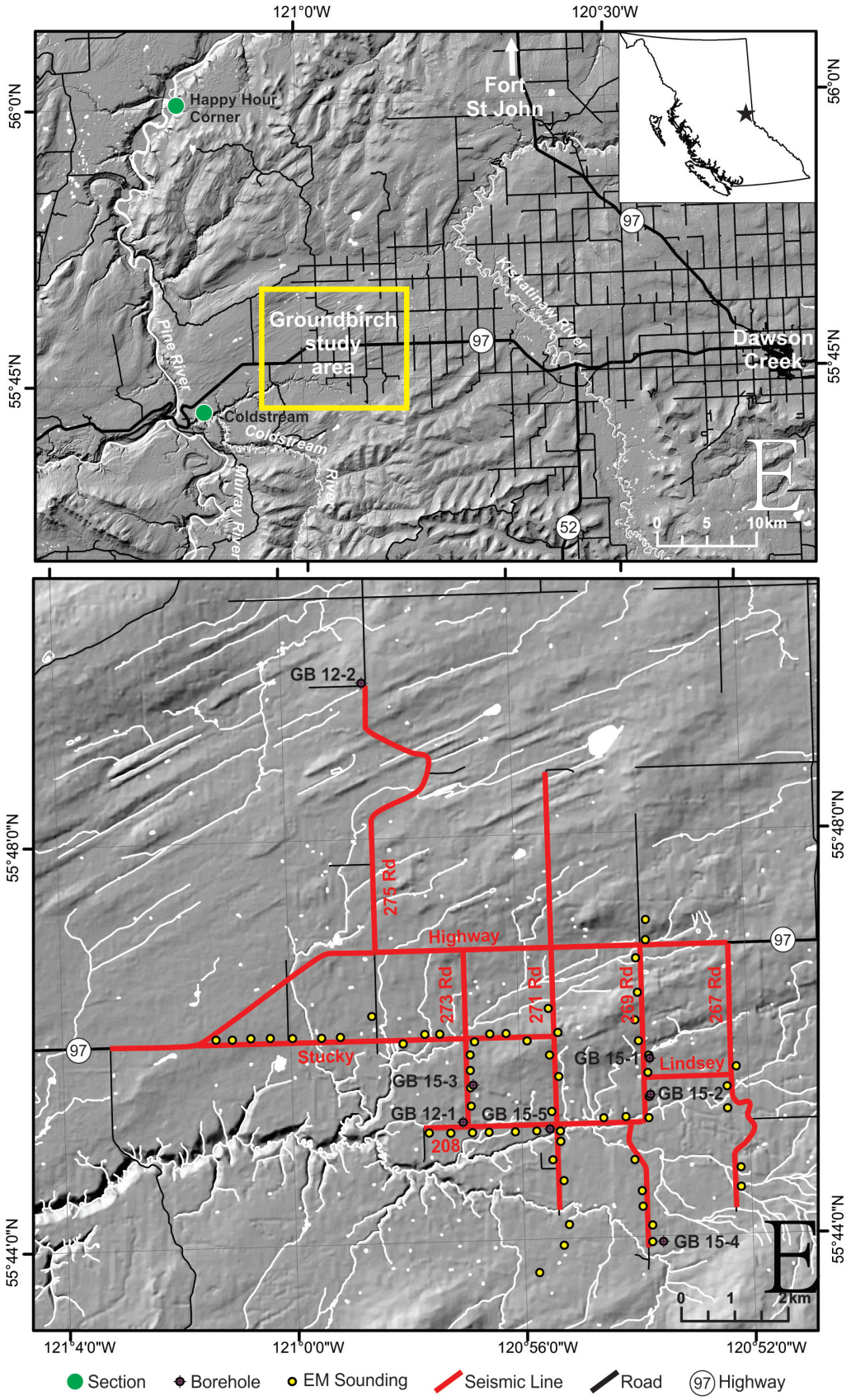

Fig. 1. Groundbirch area of northeastern British Columbia and the location of electromagnetic (EM) soundings (yellow circles) and seismic survey lines (red lines).

is integral to understanding groundwater availability. As a contribution to developing a hydrostratigraphy for future groundwater modelling, this study integrates field and drill data with ground-based electromagnetic (EM) and shallow seismic surveys to refine the geometry of, and establish a stratigraphic framework for, the buried Groundbirch paleovalley, and to highlight potential aquifers in the paleovalley.

2. Quaternary geological framework

2.1. Regional Quaternary stratigraphy

Buried Cenozoic paleovalleys are relatively common in northeastern British Columbia (Mathews, 1955, Hickin, 2011). In many cases, these paleovalleys contain Pleistocene sediments (Reimchen and Rutter, 1972; Mathews, 1978; Hickin 2013). Some paleovalleys are buried with little or no surface expression (e.g., Pawlowicz et al., 2005, 2007; Hickin et al., 2008; Ahmad et al., 2009), whereas others, like those in the study area, are in modern topographic valleys that may or may not be significant rivers courses (Mathews, 1978). Since deglaciation, many of these paleovalleys have been incised 150-250 m, exposing sediments of the paleovalley-fill succession and bedrock. Thirteen paleovalleys are known in the South Peace region (Fig. 2; Hickin, 2011; Hickin and Best, 2012).

Exposures along the Murray and Pine rivers enabled Hickin (2013) and Hickin et al. (in press) to develop a regional Quaternary stratigraphy for the south Peace area (Fig. 3). Below we describe and interpret 12 lithostratigraphic units (after Hickin, 2013; Hickin et al., in press). Each unit is assigned to a marine isotopic stage (MIS) for global age reference (Cohen and Gibbard, 2011).

2.1.1.Unit 1, non-glacial (?) - MIS 5e (?)

Unit 1 consists of indurated and oxidized bedded sand and gravel overlain by laminated sand and silt. The sediments are over consolidated and display significant large-scale deformation including 2 to 5 m-scale folds and crosscutting high-angle normal faults. Clasts are well rounded and of predominantly resistant lithologies, such as quartzite and siliceous sedimentary rocks of western provenance. Striated and faceted clasts are notably lacking. The basal contact is below river level. The unit likely records fluvial gravel bars and overbank deposits (cf. Miall, 2006). The relative age of Unit 1 is ambiguous because it is stratigraphically isolated, but the indurated and oxidized nature of the sediments suggests antiquity.

2.1.2. Units 2-4, penultimate glacial event - MIS 4 (?)

Units 2–4 are interpreted to have been deposited as a consequence of the pre-Middle Wisconsinan glacial event, probably equivalent to MIS 4. Unit 2 consists of poorly sorted, massive to weakly horizontally stratified pebble to cobble gravels. The clast-matrix ratio decreases upsection, and clast-supported gravels transition upward to matrix-supported gravels. Poorly developed m-scale bedding is marked by subtle variations in modal clast size. Clasts are subrounded to well rounded and many are striated and faceted. Clasts are of western provenance, likely from local sources and from the Main Ranges of the Rocky Mountains. The lower contact is covered; at the upper contact, the gravels grade conformably to diamicts of Unit 3. Unit 2 is interpreted to be an advance-phase glaciofluvial deposit (cf. Miall, 2006; Eyles and Eyles, 2010).

Unit 3 consists of diamict deposits that we assign to two subunits. Both subunits contain abundant faceted and striated clasts, and both contain clasts (pebbles to boulders) of mainly sedimentary rocks derived from local and western sources, and both lack clasts sourced from the Canadian Shield to the east. Subunit 3a consists of massive to weakly stratified, matrix-supported (silt- and clay-rich) diamict with abundant sand and gravel lenses. The diamict is dense and blocky and exhibits a well-developed fissility. Clasts are generally subrounded to well rounded. The diamict contains folded and thrusted sand and gravel rafts that are 1-2 m thick and extend laterally for 10s of m. These rafts likely represent fluvial and colluvial deposits that were disrupted and incorporated into the diamict by glaciotectonic processes (cf. Occhietti, 1973; Aber and Ber, 2007). Near the base of the subunit are zones in which m-scale blocks of local bedrock, diamict, and boulders are concentrated, forming, what we interpret to be a glaciotectonic mélange. Although we interpret unit 3a as a glacial deposit, it remains unclear the extent to which the diamicts were deposited directly by ice unmodified by fluvial or mass-flow processes (primary till as defined by Dreimanis, 1988). Subunit 3b, consists of massive, matrix-supported diamict with only rare, thin (< 1 cm) lenses of sand, and is likely a primary till.

Abruptly overlying unit 3, unit 4 contains beds of massive to laminated fine-grained sand, silt and clay with abundant isolated pebbles (probably dropstones). We interpret unit 4 as a glaciolacustrine deposit formed during the retreat phase of the penultimate glacial interval.

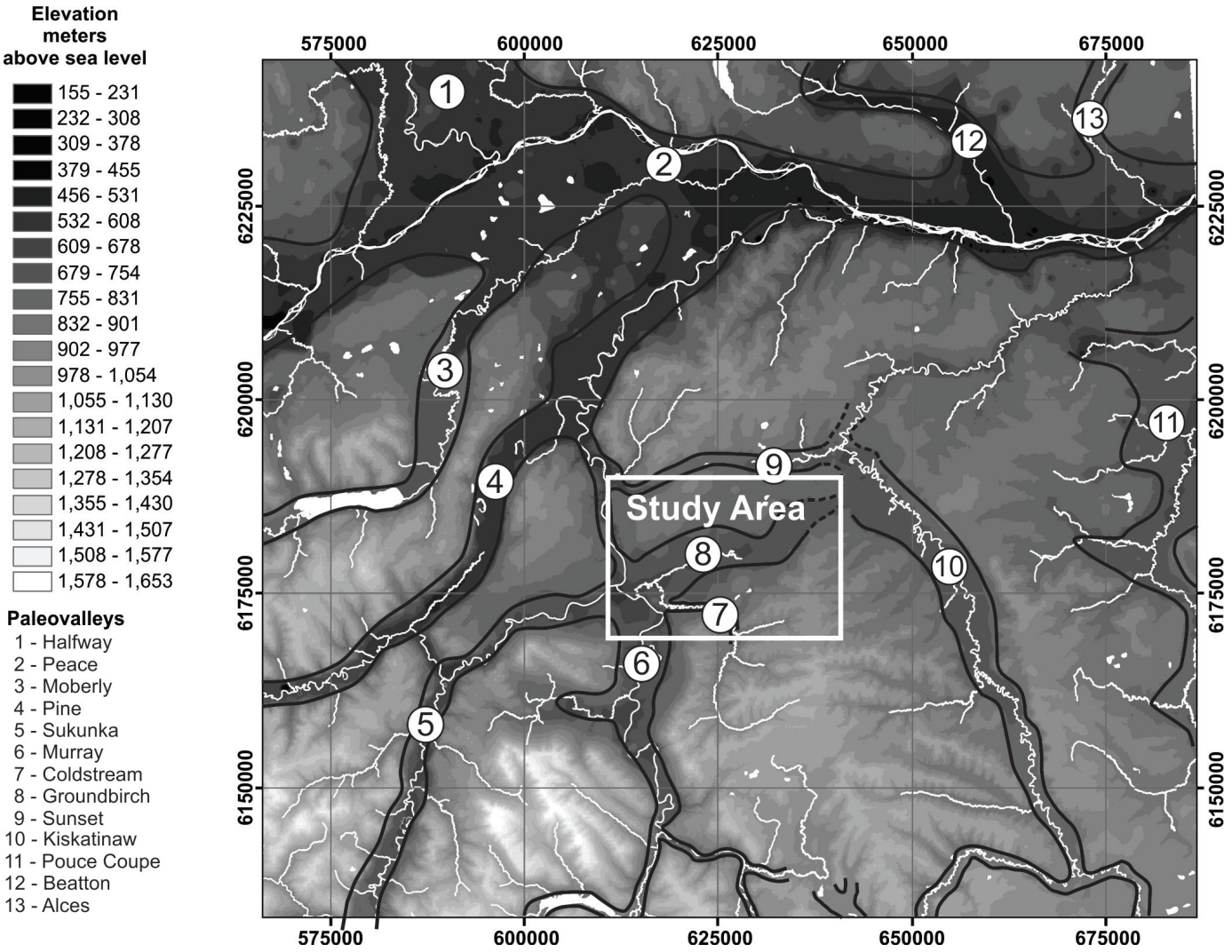

Fig. 2. The Groundbirch paleovalley is one of several buried paleovalleys mapped from water well logs and exposures in the region. Modified from (Hickin, 2011).

2.1.3. Unit 5, Middle Wisconsinan event - MIS 3

Unit 5 occurs as: 1) a heavily oxidized, partially cemented, massive to trough crossed-stratified (troughs 1-2 m wide and 0.5-1.0 m thick), open and closed-framework sand and poorly sorted pebble to cobble gravel; or 2) a massive to imbricated, clast-supported, moderately sorted, cobble gravel that fines upward to laminated sand, silt and clay, and is capped by a thin (0.5 cm) organic horizon. Unit 5 is interpreted to be a non-glacial, fluvial deposit (cf. Miall, 2006). The organic horizon, likely an overbank deposit, contains peat that was radiocarbon and optically dated as late Middle Wisconsinan (Hickin, 2013; Hickin et al., in press).

2.1.4. Units 6-11, Late Wisconsinan glacial event - MIS 2

The Late Wisconsinan glacial event (Fraser Glaciation; equivalent to MIS 2) is represented by units 6–11. Unit 6a consists mainly of oxidized, moderately to poorly sorted, clast-supported gravels. The clasts are set in a coarse- to medium sand matrix and are locally imbricated. The gravels define massive, subhorizontally stratified, and rarely cross-stratified sheet deposits and contain minor subhorizontal sand interbeds. The lower contact is erosional. Unit 6b is generally oxidized, weakly imbricated, massive to poorly stratified, poorly sorted, clast-supported pebble to cobble gravel with a fine sand, silt, and clay matrix. Clasts consist mainly of durable siliceous lithologies and are well rounded, although many are faceted and striated. The lower contact is sharp and erosional. Unit 6 is interpreted to be an advance-phase glaciofluvial deposit (cf. Eyles and Eyles, 2010).

Unit 7 consists mainly of horizontally bedded, uniform medium sand and tends to form cliffs. It is < 1 m thick south of the study area but thickens northward to more

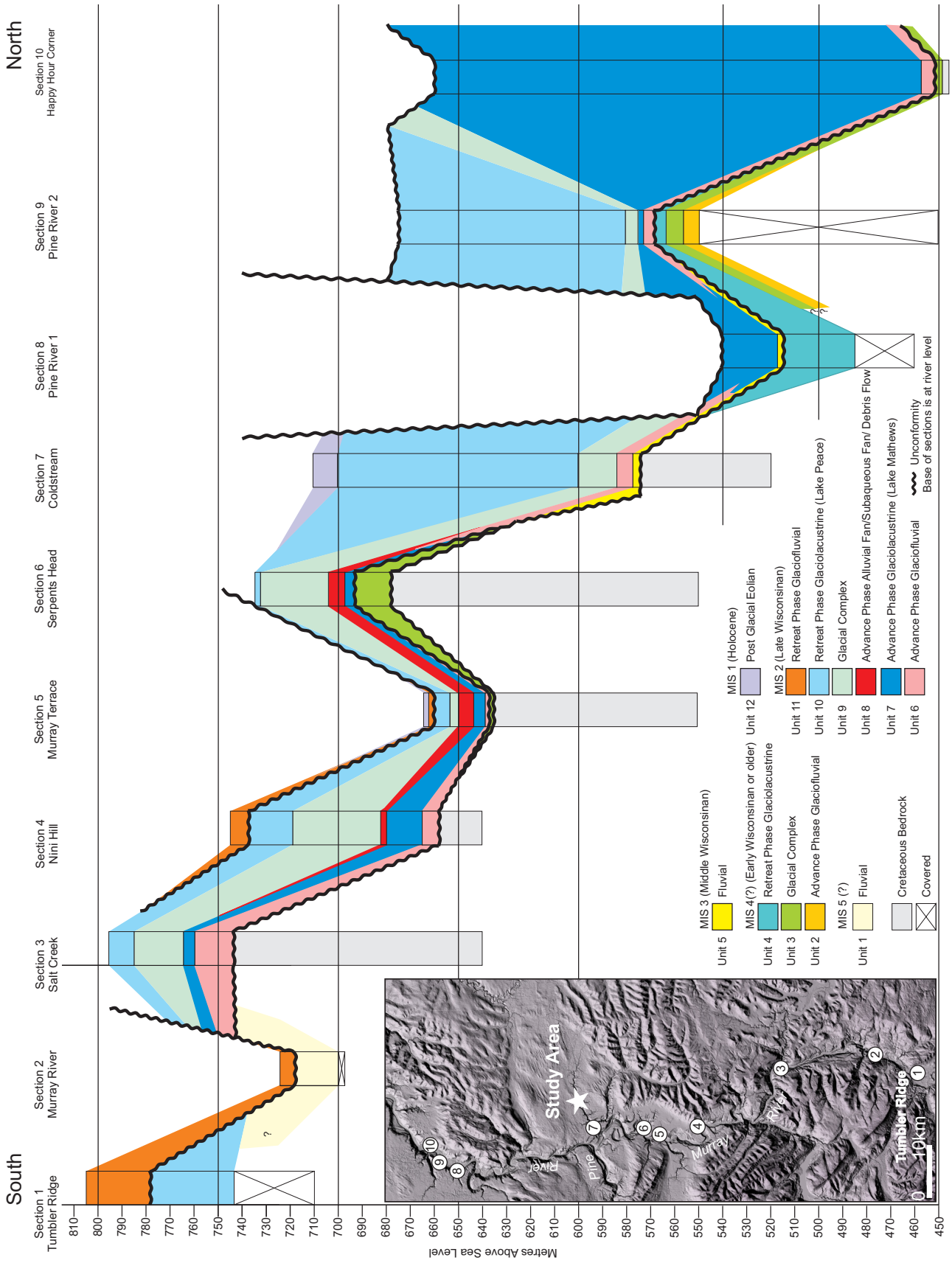

Fig. 3. South to north cross section of the regional stratigraphy exposed in the Murray-Pine river valleys. Modified from Hickin (2013).

than 200 m near the Peace River Valley. In most places the unit coarsens upward, commonly transitioning into gravel or diamict. The lower contact is conformable and gradational over about 1 m. Typically, unit 7 is finer grained in the Pine River Valley than in the Murray River Valley. Where the unit is thickest (e.g., section 10, Fig. 3), it fines up from horizontally laminated sand to laminated silt and sand (a 2-4 m thick gravel bed occurs at ~515 m asl). The unit continues to fine upward to laminated silt and clay to about 550 m asl, at which point it begins to coarsen upward (laminated silt and sand). Toward the top of the section, dropstones and thin lenses of diamict (0.1-0.4 m thick) with Shield clasts sourced from the Laurentide Ice Sheet become common. At sections 5 and 6, this unit is pervasively deformed showing both folds and faults. We interpret Unit 7 to have been deposited in an advance-phase proglacial lake, locally referred to as glacial Lake Mathews (Hartman and Clague, 2008).

Unit 8 consists of two subunits. Clasts in both subunits are of western provenance; Shield clasts are lacking. This unit consists of poorly sorted, low-angle cross-stratified to subhorizontally-stratified, pebble to cobble gravel with minor sand interbeds. The gravels are poorly sorted, and predominantly clast supported, typically with a coarse- to fine- sand matrix. Open framework gravels are locally developed. Major beds are massive; however, where they transition to sand, they display normal graded bedding. Tabular clasts are commonly flat lying or display local imbrication. Clasts are a mix of well-rounded to angular fragments. Many tabular clasts were derived from local sandstone bedrock, but exotic well-rounded quartzite and siliceous mudstone clasts are also common. The lower contact is gradational over 5-10 m, as defined by fine-grained intercalations of Unit 7. The upper contact with diamicts of Unit 9 is abrupt but conformable. Unit 8b consists of massive to weakly normally graded, clast-supported pebble to boulder diamict. Clasts are angular to sub-rounded. The matrix is clay, silt and sand and the lower contact is sharp and erosional. We interpret that Unit 8 records sedimentation from mass wasting of unstable slopes (c.f. Hooke, 1967) that flanked the proglacial lake represented by unit 7. The diverse textures and structures of the unit likely represent a continuum of depositional processes, from waterlain sheetflood sedimentation to sediment-charged mass flows, such as described from elsewhere by Lowe (1979) and Smith and Lowe (1991). Unit 8 displays a wedge-shaped geometry along the 1.5 km exposure at section 6, suggesting sedimentation, in part, as alluvial fans or fan deltas. Diamict lenses near the top of Unit 7 were probably deposited by flows that decelerated upon entering standing water.

Unit 9 consists of two subunits that are genetically distinct but grouped because they are interpreted to belong to a continuum of genetically related deposits. Unit 9a is below unit 9b and consists of stratified diamict, interbedded with horizontally laminated or massive sand. The diamict is poorly sorted, silt to clay-rich, and matrix supported. Clasts are generally subangular to well-rounded and are commonly striated and faceted. Sand horizons range from a few mm to more than 10 cm thick, and exhibit a variety of sedimentary structures, including subhorizontal stratification and ripple cross stratification. This unit is intensely deformed at section 6 where laminated sand, silt, diamict and pebble-gravel show chevron and tight to isoclinal folds with attenuated limbs that commonly merge into subhorizontal to low-angle shear zones. The lower contact of this unit is indistinct and gradational over 5-10 m and is commonly intercalated with Unit 8. Unit 9b, the more common subunit and consists of massive, poorly-sorted diamict that lacks sand and gravel interbeds. The unit generally has a silt- to clay-rich matrix with clasts that range from granules to boulders. Clasts are subangular to well rounded, commonly striated and faceted, and are a mix of local and western lithologies. Well-developed fissility is common. The lower contact is sharp and erosional at most locations but is conformable and intercalated where it overlies Unit 8. Unit 9 is interpreted to be part of a glaciogenic complex. Unit 9a is interpreted to represent a waterlain glaciogenic diamict that was glaciotectonized (at least at section 6). Unit 9b is considered a subglacial till (Hickin, 2013).

Unit 10 typically forms the surface unit in the Peace region below approximately 1000 m asl. Although the unit generally consists of clay, silt, and sand, grain-size varies across the region and within the succession (Hickin et al 2015). It ranges from a few metres to over 100 m thick. At the southern end of the study area, the unit coarsens up from rhythmically laminated silt and clay with rare pebble dropstones to horizontally stratified and ripple cross-stratified sands. In the fine-grained lower part of this unit, soft-sediment deformation features (e.g., flame structures, and dish and pillar structures) and partial and complete Bouma sequences are common. At some locations in the Murray River Valley, sands in the upper part of the unit display well-developed Type A and Type B climbing ripples (cf. Ashley et al., 1982). Near Groundbirch, Unit 10 generally fines upward; the lower unit is predominantly sand with ripple-drift cross stratification and some gravel, but fines upward to rhythmically bedded silt and sand with abundant thinly

bedded diamict and common dropstones, which become rarer towards the top. Unit 10 is interpreted to represent deposition in a retreat-phase proglacial Lake Peace (Mathews, 1980; Hickin et al., 2015).

Unit 11 is differentiated into two subunits, both of which consist of gravel and sand. The unit typically forms the surface unit on most terraces along the river valleys, except where Unit 12 is present. Clasts of both sub-units have western sources and are moderately to well-rounded and commonly faceted. Striations are common on cobbles and boulders. Large-scale (2-4 m thick) planar tabular crossbeds distinguishes this unit from unit 11b. Unit 11b consists of pebble to cobble gravel with interbedded sand that is overlain by horizontally stratified silt and sand. The gravel can be massive or crudely bedded, poorly to well sorted, has open and closed frameworks, and is poorly to well imbricated. Clasts are moderately to well-rounded and facets are common. Planar and trough cross bedding is also common. Silts and sands in the upper part of the unit are horizontally laminated to thinly bedded. Although typically 1-2 m thick, the unit may be > 4 m thick. The large-scale planar cross strata in Unit 11a are interpreted to be foresets of glaciofluvial deltas formed during stable phases of glacial Lake Peace. Unit 11b is interpreted to be retreat phase glaciofluvial deposits representing the fluvial equivalent of Unit 11a deposited between the retreating ice front and margins of glacial Lake Peace.

2.1.5. Unit 12, Holocene - MIS 1

Unit 12 consists of massive to poorly stratified, moderately sorted silt and fine sand. Unit 12b, exposed at several locations along terraces where Unit 12a is present, consists of oxidized, uniform medium sands that form parabolic sand dunes. All of unit 12 is considered eolian.

2.2. Stratigraphy of Groundbirch paleovalley

The Groundbirch paleovalley, which was originally identified by Callan (1970), hosts a major local aquifer (Lowen, 2011). Although Cowen (1998) considered the Groundbirch paleovalley as a tributary of the Kiskatinaw paleovalley that drained eastward, Hickin (2011) showed that it is a tributary of the Murray-Pine paleovalley system (Fig. 2). Cowen (1998) reported good-quality fresh water hosted in “interglacial sand and gravel.” His test drilling indicates that the local stratigraphy differs from that presented by Callan (1970). In particular, the test drilling failed to intersect the basal gravel (aquifer) expected at the bedrock-sediment contact, which suggests that the aquifer(s) may be discontinuous or occur at different stratigraphic levels. The bedrock topographic model by Hickin (2011) from water well data suggested that the Groundbirch paleovalley is approximately 6 km wide and 100 m deep, and trends east-northeast from the Kiskatinaw River to the Pine-Murray river confluence. Based on an unconstrained EM survey, Hickin and Best (2013) suggested that the valley is 3-4 km wide and about 100 m deep. Seismic and drilling data from the present study indicates the paleovalley is much deeper (>300m).

The stratigraphy of the Groundbirch paleovalley is documented in Hickin (2013), after which the following is summarized. The lower succession is exposed at Happy Hour Corner on the Pine River (Fig. 4). The upper succession is exposed at the mouth of the Coldstream River and along Sheep Creek (Fig. 5).

2.2.1. Happy Hour Corner section

The Happy Hour Corner section (Fig. 4) is exposed along the Pine River, 30 km north of the confluence of the Pine and Murray rivers (Fig. 1). Shales of the Shaftesbury Formation (Cretaceous; McMechan, 1994) are exposed at river level. These shales are overlain by a >200 m-thick section of Quaternary sediments, most of which are interpreted to have been deposited beneath tills of the Fraser glaciation (Late Wisconsinan; Hickin, 2013). The lowest unit (0.5 to 15 m thick) is a matrix-supported diamict with large rafts of sand and gravel, which is considered part of Unit 3 (see above; Hickin, 2013) and interpreted to be part of a penultimate glacial complex. At this section, Unit 3 is overlain by massive clast- and matrix-supported gravel that fines upwards to planar cross-bedded sand with intercalated clast-supported gravel, interpreted to be part of Unit 6, the advance phase glaciofluvial deposit. Unit 6 is conformably overlain by Unit 7, which consists of horizontally stratified sand, that fines upward to rhythmically laminated sand silt and clay. Unit 7 is more than 100 m thick, contains abundant dropstones and diamict lenses in its upper levels, and is interpreted to be part of an advance phase glaciolacustrine deposit (glacial Lake Mathews).

2.2.2. Coldstream River section

Exposed along a 3 km stretch of the canyon at the mouth of Coldstream River (Fig. 1) is a nearly continuous 170-m thick section of valley-fill sediments and underlying bedrock (Fig. 5). The base of the section is represented by Cretaceous bedrock including mudstones of the Kaskapau Formation and mudstones and fine sandstones of the Dunvegan Formation (Stott,

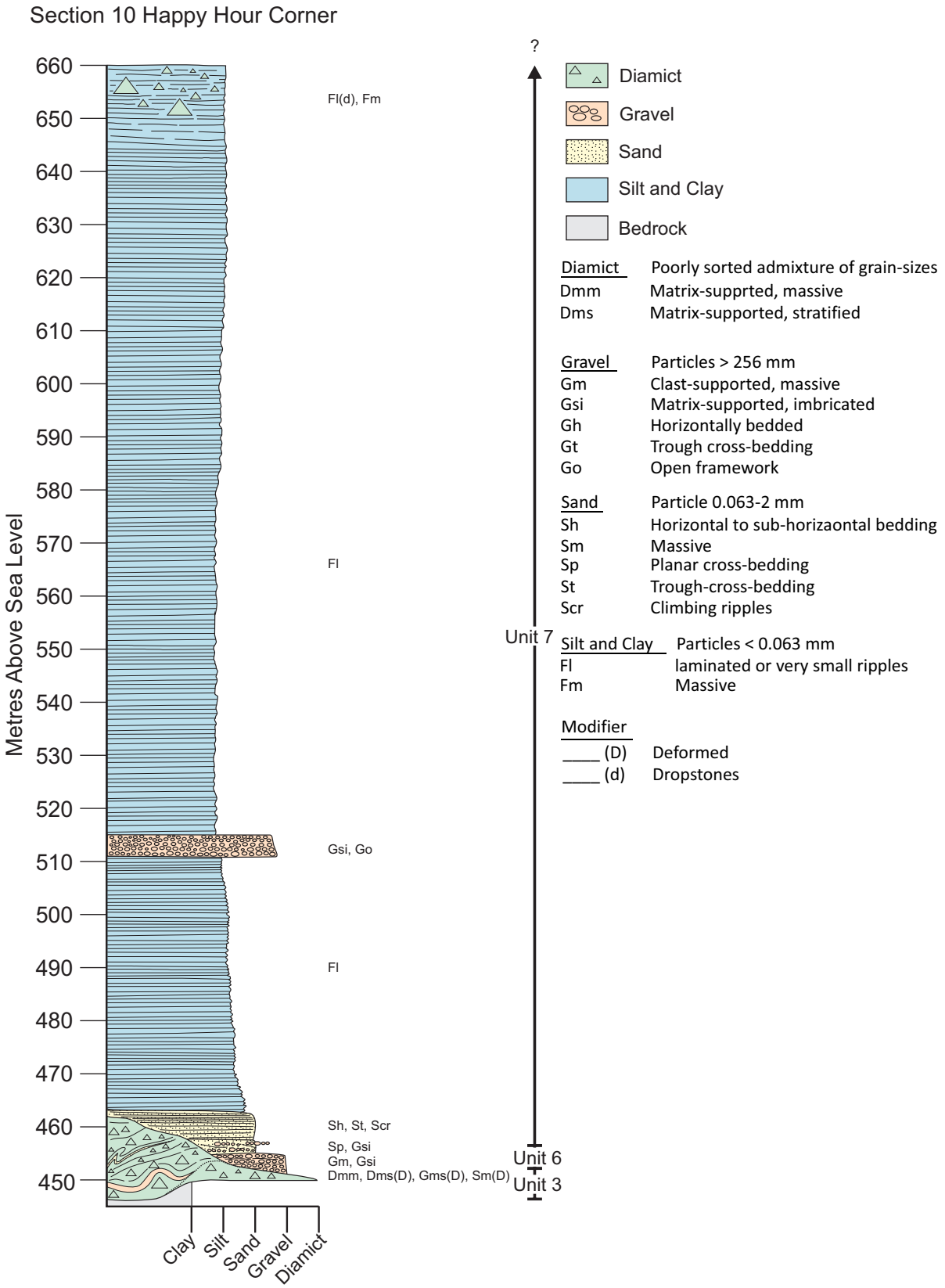

Fig. 4. Stratigraphy exposed at the Happy Hour Corner Section (section 10; see Fig. 1 for location) along the Pine River. Most of the section consists of Unit 7 sand and gravels, advance phase glaciolacustrine deposits of glacial Lake Mathews. Modified from Hickin (2013).

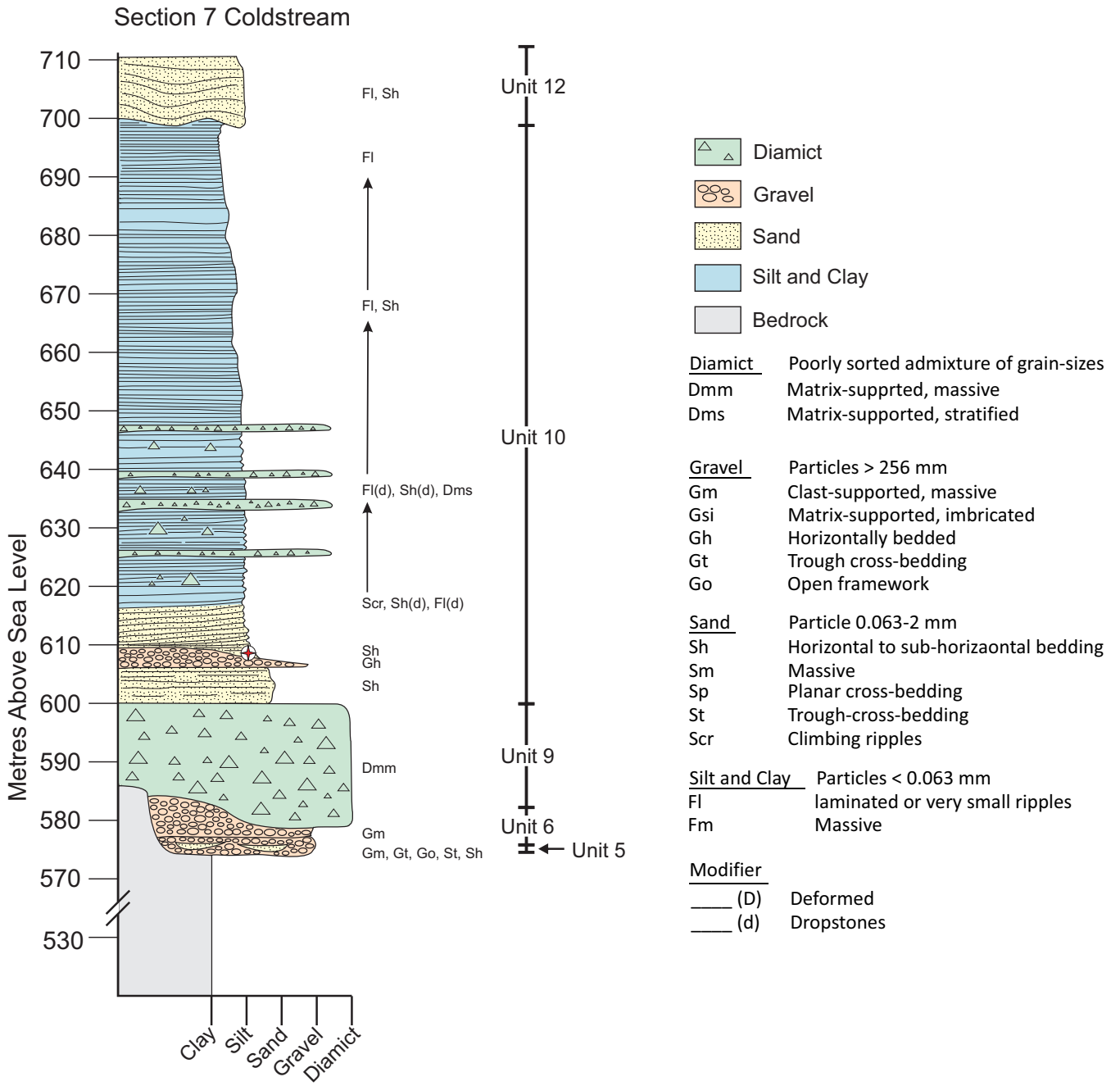

Fig. 5. Stratigraphy exposed at the Coldstream section (section 7; see Fig. 1 for location). Modified from Hickin (2013).

1961; McMechan, 1994). Dunvegan Formation rocks at the base of the Coldstream River canyon include flat-lying, well-bedded, recessive fine-grained mudstone with 1-2 m thick resistant sandstone interbeds.

Although poorly exposed, the lowest unconsolidated unit consists of fluvial sand and gravel that we consider pre-glacial or interglacial fluvial deposits equivalent to Unit 5. It consists of partially cemented, oxidized and indurated interbeds of trough cross-bedded sand and gravel. At this section, Unit 5 is overlain by clast-supported, moderately oxidized, poorly sorted, pebble- to cobble gravel in a silt to granule matrix equivalent to Unit 6. Unit 6 forms discontinuous lenses up to 6 m thick, and is interpreted to be a non-glacial fluvial deposit that transitions upwards into an advance phase glaciofluvial deposit. Unit 8 overlies Unit 6 and consists of matrix-supported, poorly sorted, granule to boulder diamict that is interpreted to be a till deposited during the Fraser Glaciation (Late Wisconsinan). The unit is 12-20 m thick and is regionally extensive. Unit 8 is overlain by a

discontinuous horizon (about 10 m thick) at the base of Unit 10 consisting of medium sand that coarsens upward to gravel. It is interpreted to represent an ice contact, subglacial fluvial succession that was deposited into glacial Lake Peace. The upper part of Unit 10, which constitutes most of the Coldstream section, is a regionally extensive glaciolacustrine succession deposited in glacial Lake Peace. It generally fines upwards and consists of well-bedded, horizontally stratified clay, silt, sand and diamict. The top of the Coldstream section includes 6 m of silty sand interpreted to be equivalent to eolian deposits of Unit 12.

3. Methods and results

The validity of hydrogeological models depends on the quality and distribution of data from which they are derived. Critical inputs are the geological framework and lithologic characteristics, which are key parameters for groundwater storage and flow (Freeze and Cherry, 1979). Where the distribution and quality of well data are insufficient to provide an appropriate geological framework, geophysical methods are an alternative for geological control. As Van Dam (2012) noted, the interpretation of geophysical datasets is enhanced when two or more complimentary geophysical data sets are available. For example in northeastern British Columbia, Hickin et al. (2009) used a combination of ground penetrating radar and capacitive-coupled resistivity to investigate the structure and texture of a floodplain deposit. Similarly, Ahmad et al. (2009) used high-resolution seismic and resistivity to profile a buried paleovalley in northwest Alberta. More recently, the Geological Survey of Canada has combined its high-resolution shallow seismic data with other airborne and ground based EM and resistivity data to investigate paleovalley geometry, stratigraphy and aquifer potential (e.g., Oldenborger et al., 2013; Pugin et al., 2014; Sapia et al., 2015). In this study, we integrate drilling with ground-based electromagnetic (EM) and shallow seismic surveys. EM data from Hickin and Best (2013) are reprocessed using reflections from a shallow seismic survey to constrain 1-D inversions.

3.1. Drilling, coring, and downhole geophysical methods

Two drills were used to collect core from 5 sites (Table 1). Boreholes GB 15-1 and GB 15-2 were drilled using a mobile B-54 track mounted, multi-purpose drill rig capable of auguring (hollow and solid stem), mud rotary, air rotary and diamond coring (rock and soil). Where the substrate was competent (i.e., fine sediment, till, and bedrock) HQ cores (diameter: 63.5 mm) were cut with a diamond drill head. Where substrate was saturated or too coarse to core (i.e., sand or gravel), the borehole was extended with a mud rotary tri-cone bit. Although core was not recoverable when using a tri-cone drill bit, the cuttings were ejected with the mud, then washed and examined to determine lithology and, in combination with driller's feedback (i.e., drilling speed, drilling pressure, and drill behavior) to speculate on clast size.

Boreholes GB 15-3 to GB 15-5 were drilled with a Sonic ATV L600. Sonic cores were collected by advancing 4- inch (10.2 cm) casing 10-20 feet (3.04-6.10 m) at a time. A 6-inch (15.2 cm) override casing was then advanced behind the 4-inch casing to depth. The 4-inch casing was then retracted and pulled to the surface where water pressure was used to push the core sample out of the 4- inch casing into clear tubular bags for placement in core boxes.

All wells were completed with grouted 3-inch (7.6 cm) schedule 80 PVC. PVC casing permits collecting electrical downhole geophysical data and non-muted gamma logs. Logs were collected in three separate logging descents via wireline to petroleum industry open-hole data standards. We used the following Weatherford *Compact*^{TM} tools:

Table 1. Drill hole locations and information.

Drill Hole	Lat.	Long.	Easting* (UTM)	Northing* (UTM)	Coring Method	Total Depth (m)
GB 15-1	55°45'44.7"	120°53'51.5"	631912	6181638	HQ Diamond	82.3
GB 15-2	55°45'20.3"	120°53'50.6"	631949	6180885	HQ Diamond	146.3
GB 15-3	55°45'26.2"	120°56'57.1"	628694	6180970	Sonic	68.9
GB 15-4	55°43'57.8"	120°53'37.1"	632263	6178341	Sonic	70.7
GB 15-5	55°45'04.8"	120°55'25.1"	630318	6180355	Sonic	118.0

*Universal Transverse Mercator (UTM) zone 10, North American Datum (NAD) 83

Compact™ Gamma Ray (MCG and auxiliary unit MGS), Compact™ Two-Arm Caliper (MTC), Compact™ Array Induction (MAI), Compact™ Focused Electric (MFE), Compact™ Photodensity (MPD), Compact™ Dual Neutron (MDN), and Compact™ Sonic Sonde (MSS). Typical drilling mud resistivity of 2 Ωm and density of 1000 kg/m^3 was assumed. All logging tools were within calibration tolerances at the time of logging.

Gamma ray logs measure the natural radioactivity of the sediment and is measured in American Petroleum Institute (API) units (i.e., a calibrated unit from an artificially radioactive concrete block at the University of Texas). In general, high gamma values reflect clay-rich deposits and low gamma values are from coarse-grained units.

The sonic log measured the P-wave slowness (1/velocity) with units of microseconds per metre (μs/m). These logs were converted to m/s for direct comparison with the P-wave seismic velocity. The S-wave sonic log was not obtained, so comparisons between the seismic S-wave velocity and the S-wave sonic velocity were not made. The reflection coefficient (R) at the interface between two geological units (at normal incidence) is:

$$R = (\rho_2 v_2 - \rho_1 v_1)/ (\rho_2 v_2 + \rho_1 v_1)$$

where:

ρ = density in kg/m^3
v = velocity in m/s.

The product of density and velocity (ρv) is called the acoustic impedance. The unit above the interface is unit 1 and the unit below the interface is unit 2. Generally, density variations between consolidated and unconsolidated sedimentary deposits are much smaller than the corresponding velocity variations. Consequently the acoustic impedance is mostly controlled by velocity variations in these deposits.

The ability of sediment to conduct electricity depends on the volume of pore space and clay content. In general, sand and gravel with fresh water or air-filled pores will have high resistivity, whereas fine-grained sediment with small pores and abundant clay will have low resistivity.

3.2. Drilling, coring, and downhole geophysical results

The diamond coring was generally effective in moist silt, dense sediment such as till, or bedrock, but was problematic in saturated and coarse-grained material such as gravel. Core recovery was poor in the finest material at the top of the wells or in dry sand that jammed in the core barrel and, when compacted, prevented subsequent material entry. Saturated sand was also difficult to recover; between about 30 and 35 m, the integrity of the wellbore wall was compromised by heaving sand and collapse of the wellbore wall, and the drill string needed to be flushed and cleaned repeatedly. Recovery in gravel was also limited because of clasts larger than the diameter of the coring tool. Consequently, the zone between 35 and 60 m, which hosts a major fresh water aquifer, was cased and core was not recovered. Nonetheless, enough discontinuous core was recovered to characterize the lithologic units.

The sonic drilling was faster than the diamond drilling and yielded better recovery (75-100% in some intervals). However, in the saturated gravel, recovery was locally limited to about 60%. The length of recovered core was commonly >100% due to capture of lost core from the previous interval as well as swelling of core, particularly in till. When lost core in any one interval was recovered at the top of the subsequent core interval, it was invariably a saturated slurry, with too much drilling water to provide a meaningful log.

Below are summaries of the well logs. Detailed log descriptions are provided in Appendix A. All down hole geophysical data files are in Appendix B.

3.2.1. GB 15-1

Borehole GB 15-1 was drilled on the west side of the 269 Road, 2.1 km south of Highway 97 (Fig. 1). The well was drilled on the north flank of the paleovalley to a depth of about 113 m (605 m asl) and intersected bedrock at about 81 m (637 m asl; Fig. 6a). The bedrock is laminated mudstone (Fig. 6b). At the bedrock-Quaternary sediment contact is a zone of breccia in which bedrock clasts are separated by fine-grained sediment (Figs. 6c, d). This fine-grained sediment extends as bedding-concordant and bedding-oblique seams for up to 5 m beneath the contact. The lowest unconsolidated unit is approximately 3 m thick and consists of laminated clay, silt, and very fine- to medium-sand (Fig. 6e). This unit is interpreted to have be deposited in standing water and is assigned to Unit 7 (Hickin, 2013), the advance phase glaciolacustrine deposits of glacial Lake Mathews. We interpret that the zone of breccia at the bedrock-sediment contact formed by forceful injection due to ice loading of water saturated glaciolacustrine sediments. Alternatively, sediment may have been injected under elevated hydrostatic conditions in a subglacial lake. Unit 7 is overlain by about 20 m of massive and stratified diamict (Fig. 6f) interpreted to be till and subglacial deposits of a Late Wisconsinan glacial

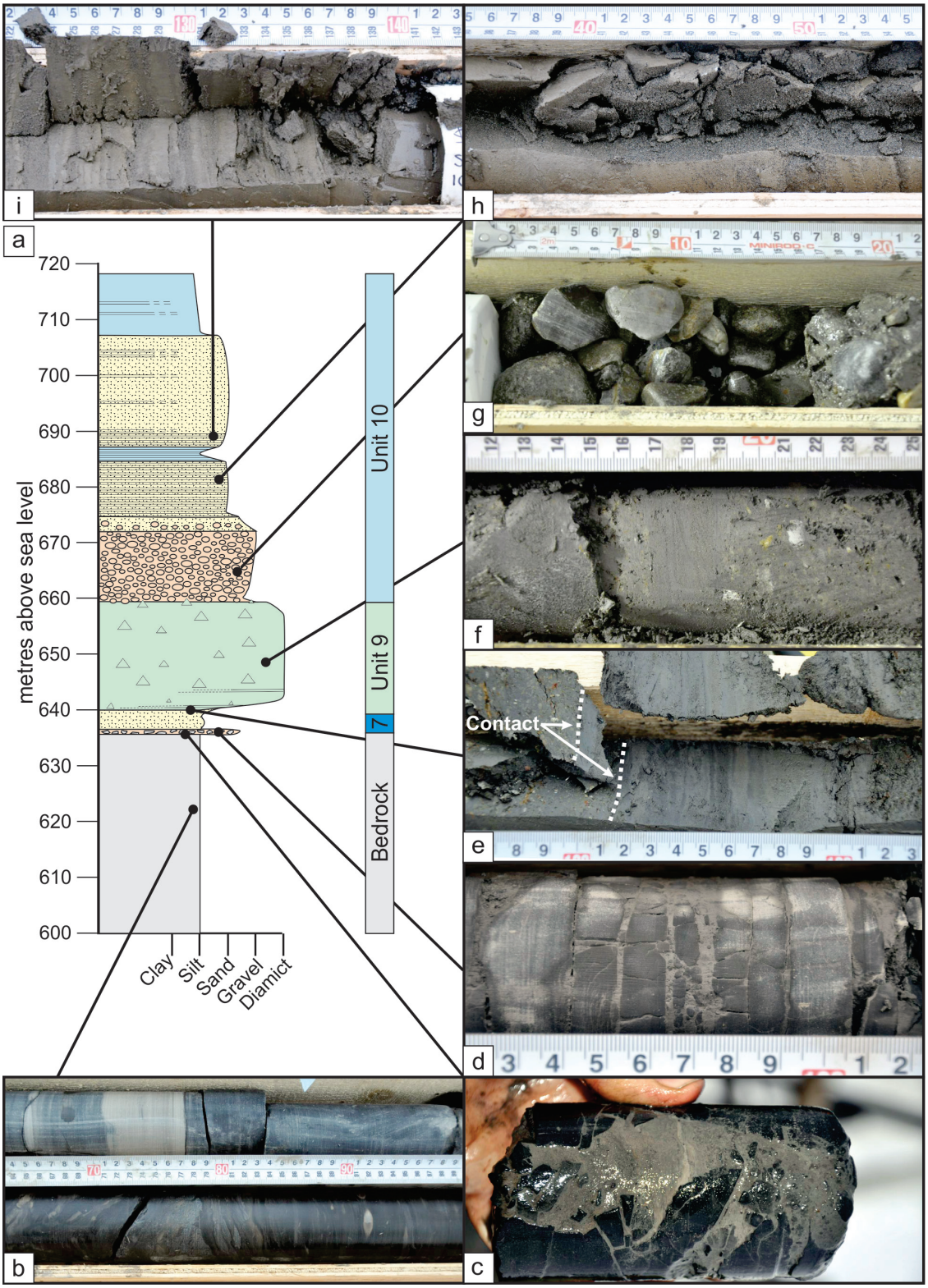

Fig. 6. Borehole GB15-1 (see Fig. 1 for location). **a)** Lithology log; **b)** Competent, bedded mudstone and fine sandstone bedrock; **c)** Breccia of bedrock fragments separated by silt and clay across bedding; **d)** Bedrock with injected silty clay along bedding; **e)** lower contact between till (Unit 9) and advance phase glaciolacustrine silt and clay (Unit 7, glacial Lake Mathews); **f)** Diamict, interpreted to be till (Unit 9); **g)** Pebble- to cobble- clasts from gravel assigned to the base of Unit 10, immediately above diamict (Unit 9); **h)** Laminated medium sand from Unit 10 (glacial Lake Peace; and **i)** Retreat phase glaciolacustrine laminated silt and sand from Unit 10 (glacial Lake Peace).

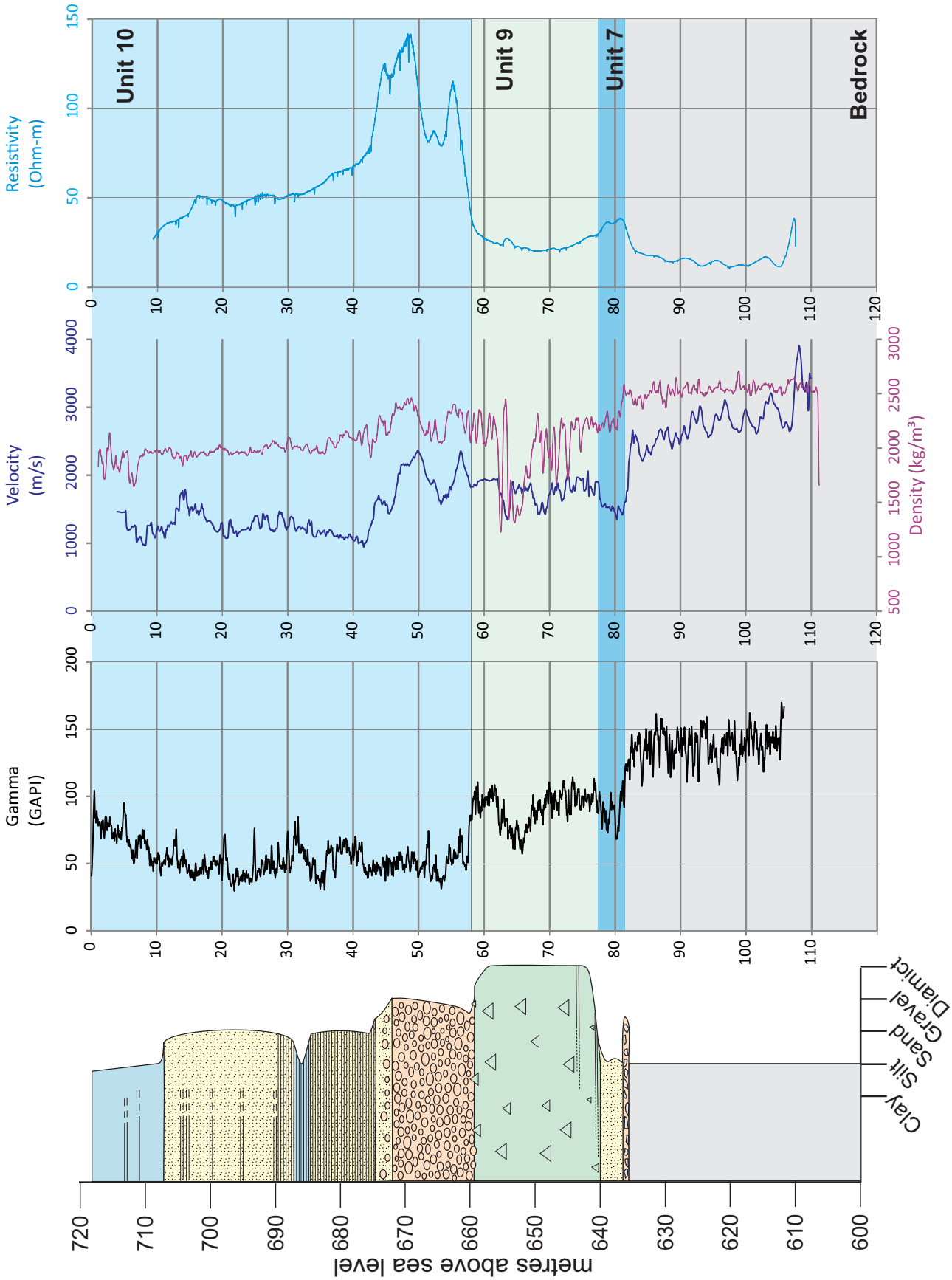

Fig. 7. Lithology log from borehole GB15-1 with gamma ray, sonic, and resistivity logs.

Table 2. Generalized unit petrophysical properties from downhole geophysics ($\bar{x}$ = mean average).

Unit	Drill Hole	Depth (m)	Elevation (m asl)	Gamma (GAPI)	Velocity (m/s)	Density (kg/m^3)	Resistivity (Ohm-m)
Unit 10 (fine)	GB15-1	0-42	718-676	30-104 $\bar{x}$ = 55	941-1786 $\bar{x}$ = 1247	1644-2215 $\bar{x}$ = 1974	27-76 $\bar{x}$ = 51
Unit 10 (coarse)	GB15-1	42-58	676-660	31-78 $\bar{x}$ = 50	1107-2366 $\bar{x}$ = 1876	1911-2461 $\bar{x}$ =2240	48-142 $\bar{x}$ = 103
Unit 9	GB15-1	58-78	660-640	55-115 $\bar{x}$ = 91	1345-2058 $\bar{x}$ = 1780	1225-1450 $\bar{x}$ = 2005	20-45 $\bar{x}$ = 25
Unit 7	GB15-1	78-82	640-635	65-125 $\bar{x}$ = 91	1350-1905 $\bar{x}$ = 1528	2145-2585 $\bar{x}$ = 2305	30-40 $\bar{x}$ = 36
Bedrock	GB15-1	82->112	635-<600	105-155 $\bar{x}$ = 139	2053-3905 $\bar{x}$ = 2775	2370-2710 $\bar{x}$ = 2545	10-20 $\bar{x}$ = 15
Unit 10	GB15-2	0-69	710-641	26-132 $\bar{x}$ = 67	996-2519 $\bar{x}$ = 1467	1454-2517 $\bar{x}$ = 2062	24-104 $\bar{x}$ = 53
Unit 9/8	GB15-2	69-93	641-617	27-100 $\bar{x}$ = 52	964-2419 $\bar{x}$ = 1393	1902-5296 $\bar{x}$ = 2107	35-101 $\bar{x}$ = 62
Unit 7	GB15-2	93->145	617-<565	34-84 $\bar{x}$ = 55	976-2200 $\bar{x}$ = 1325	1722-2147 $\bar{x}$ = 2020	38-70 $\bar{x}$ = 50
Unit 10	GB15-3	0-38	700-662	31-142 $\bar{x}$ = 79	1264-2054 $\bar{x}$ = 1625	836-2110 $\bar{x}$ = 1742	20-96 $\bar{x}$ = 46
Unit 9	GB15-3	38-55	662-645	43-138 $\bar{x}$ = 79	1793-2954 $\bar{x}$ = 2085	1706-2267 $\bar{x}$ = 2024	16-68 $\bar{x}$ = 40
Bedrock	GB15-3	55->65	645-<635	53-435 $\bar{x}$ = 113	2161-3463 $\bar{x}$ = 2656	1391-2559 $\bar{x}$ = 2248	16-30 $\bar{x}$ = 20
Unit 10	GB15-4	0-39	722-683	32-143 $\bar{x}$ = 79	1268-2187 $\bar{x}$ = 1715	882-2290 $\bar{x}$ = 1850	24-48 $\bar{x}$ = 40
Unit 9	GB15-4	39-62	683-660	41-110 $\bar{x}$ = 65	1510-2601 $\bar{x}$ = 1971	1552-2425 $\bar{x}$ = 2106	15-99 $\bar{x}$ = 43
Unit 10 (fine)	GB15-5	0-29	704-675	69-139 $\bar{x}$ = 103	1132-2054 $\bar{x}$ = 1437	884-2074 $\bar{x}$ = 1793	16-55 $\bar{x}$ = 31
Unit 10 (coarse)	GB15-5	29-46	675-658	37-86 $\bar{x}$ = 58	1604-2411 $\bar{x}$ = 2099	2082-1707 $\bar{x}$ = 2349	15-99 $\bar{x}$ = 58
Unit 9/8	GB15-5	46-60	658-644	70-109 $\bar{x}$ = 93	1313-2089 $\bar{x}$ = 1771	1933-2261 $\bar{x}$ = 2085	10-30 $\bar{x}$ = 20
Unit 7	GB15-5	60->120	644-<584	50-104 $\bar{x}$ = 70	1911-3487 $\bar{x}$ = 2649	1788-2137 $\bar{x}$ = 2012	13-87 $\bar{x}$ = 43

succession (Unit 9). The uppermost unit (assigned to unit 10) consists of a fining-upward succession of gravel (Fig. 6g) overlain by saturated, laminated to massive, very fine- to medium-sand, and capped by laminated clay, silt, and sand (Figs. 6h-i). The gravel in this part of the succession is interpreted to represent subglacial fluvial deposits discharged into an ice contact lake (glacial Lake Peace; Hickin, 2013). The sediments in the remainder of the succession are interpreted to be part of retreat phase glacial Lake Peace (Hickin et al. 2015).

Geophysical logs from GB 15-1 correlate well with the lithologic data (Fig. 7). The average gamma value of bedrock is 139 API (Table 2); across the bedrock-Unit 7 contact, this value decreases abruptly to an average of 91 API (Fig. 7). The contact between units 7 and 9 is marked by a modest increase in the gamma response to approximately 98 API (Fig. 7). Overall, Unit 9 also has an average gamma value of 91 API. However, the lower 10 m fluctuates near 98 API but drops to about 75 API between 62-67 m before increasing to about 100 API at the top of the unit. Unit 10 consists of a lower gravel (about 18 m) and an upper sand and silt succession (about 40 m). The average gamma response in the gravel is 50 API and increases upwards from as low as 30 API to about 100 API (averaging 55 API), consistent with the fining-upward grain-size trend.

Velocity in bedrock decreases upwards from about 3900 m/s to about 2000 m/s. Velocity drops to an average of about 1500 m/s through Unit 7. Unit 9 displays minor velocity fluctuations, with an average of 1700 m/s. Two distinct velocity zones in Unit 10 correlate with the lower gravel package and the upper sand and silt succession. Velocity fluctuates, but decreases through the gravel succession from about 2400 m/s to 1100 m/s. Velocity in the sand and silt succession averages about 1250 m/s.

Density in bedrock is consistent, averaging 2550 kg/m^3. Above bedrock, in Unit 7, density decreases abruptly to about 2300 kg/m^3. Density is erratic in Unit 9 (averaging 2005 kg/m^3) and through the lower gravel succession in Unit 10 (averaging about 2240 kg/m^3). Density is stable in the upper part of Unit 10, averaging about 2000 kg/m^3. Based on the velocity and density data, reflections are expected at the top of the gravel in Unit 10 and at the sediment-bedrock interface.

The mudstone bedrock, has an average resistivity of 15 Ohm-m. Resistivity increases through Unit 7 (sand) averaging 36 Ohm-m. This slight increase in resistivity, relative to the bounding units, suggests the presence of a small (3 m) fresh water aquifer. Resistivity is consistently low through Unit 9, averaging 25 Ohm-m. The gravel succession in unit 10 displays a large resistivity spike, peaking at 142 Ohm-m (average 103 Ohm-m). These data suggest that the gravel at the base of Unit 10 is an excellent target for a fresh-water aquifer. Resistivity decreases from 76 to 27 Ohm-m though the remainder of Unit 10, consistent with the fining-upward succession.

3.2.2. GB15-2

Borehole GB 15-2 is on the west side of the 269 Road, about 700 m south of GB 15-1 (~2.8 km south of Highway 97; Fig.1). This borehole was drilled to a depth of 146 m (564 m asl) and failed to intersect bedrock (Fig. 8a). The lowest unit, between 564 and 615 m asl (>51 m), initially fines-upwards from predominantly sand (Fig. 8b) to predominantly sandy silt and clay (Fig. 8c). The unit then coarsens upward to mainly silty sand (Fig. 8d). This part of the succession is interpreted to have been deposited in a low-energy standing body of water and is assigned to Unit 7 (advance phase glacial Lake Mathews; Hickin, 2013). Although core was not recovered, we speculate that this unit is overlain by 20 m of interbedded gravel (and possibly diamict), based on drill chip samples and drill behaviour (diminished drilling rate and increased 'bouncing'). However, interbedded gravel, sand, silt, clay, and diamict core was recovered from the top of the unit (Fig. 8e). We interpret the succession above Unit 7 to be polygenetic but predominantly deposited into a glaciolacustrine environment. Notably, a thick (>5 m) Late Wisconsinan till, which is the typical marker horizon for the last glacial maximum, appears to be lacking. We speculate that the interbedded gravel, sand, silt, clay, and diamict section is entirely glaciogenic and represents diverse subglacial and glaciolacustrine processes with only limited subglacial till deposition. We assign this package to a mixture of unit 8 and 9 and consider it to be part of the Late Wisconsinan glacial complex. At this location, Unit 9 is overlain by saturated medium sand (Fig. 8f) that fines upward to very fine sand and silt with rare pebbles. This is overlain by about 20 m of sand and gravel (Fig. 8g). Coring was not attempted in the saturated gravel and sand because casing was required to prevent collapse of the hole. Core was recovered from the top of the succession and generally reveals fining-upward sediments that range from fine sand (Fig. 8h) to laminated clay and silt (Fig. 8i). This unit is lithologically similar to the top of the succession described in GB 15-1, and is interpreted to record fluvial sedimentation from subglacial streams that discharged into glacial Lake Peace, followed by standing-water glaciolacustrine sedimentation (Unit 10).

Geophysical logs from GB 15-2 can be related to

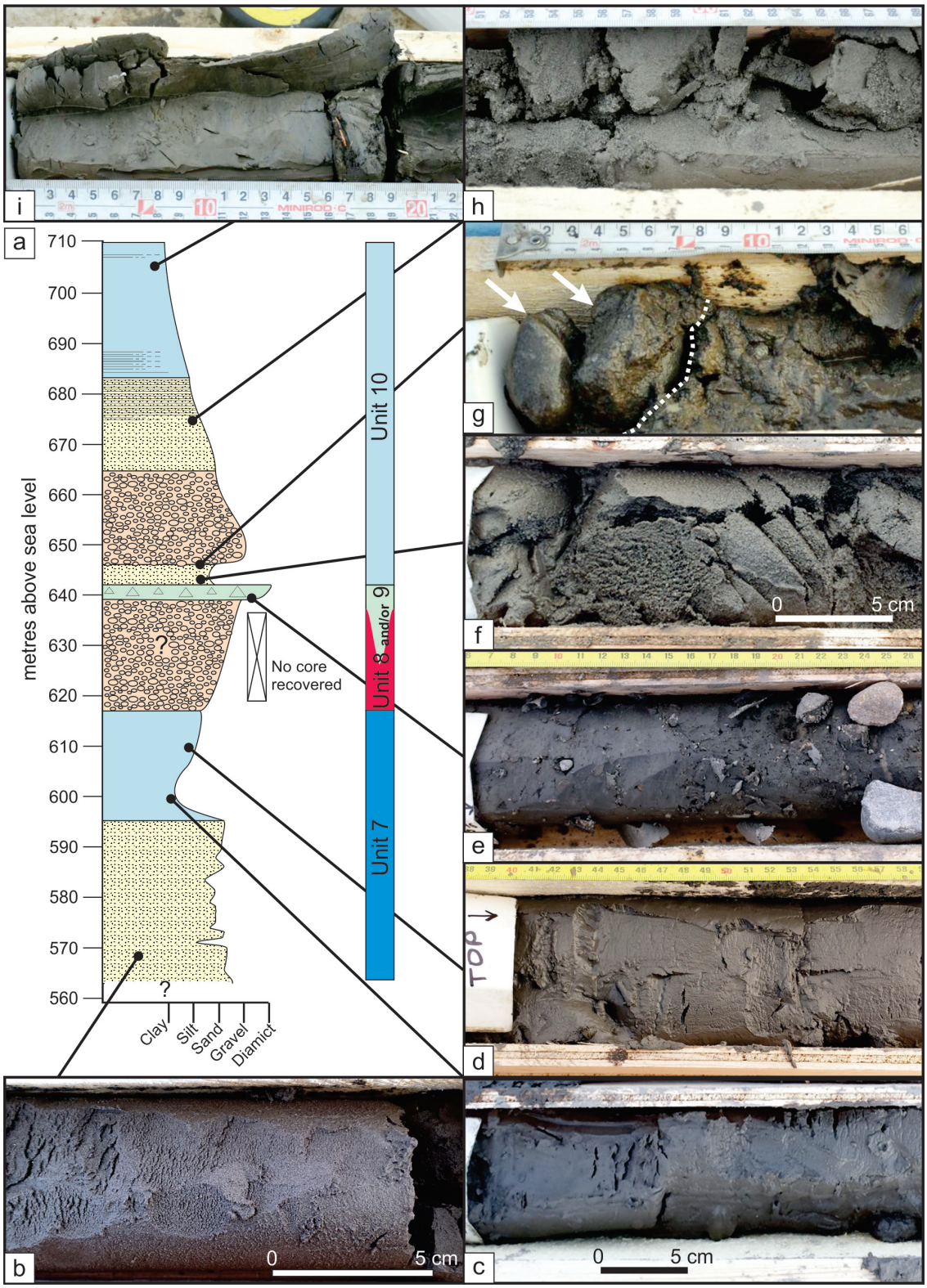

Fig. 8. Borehole GB15-2 (see Fig. 1 for location). **a)** Lithology log; **b)** Medium Sand, advance phase glaciolacustrine (unit 7); **c)** Silty-clay, advance phase glaciolacustrine (Unit 7); **d)** Silty-fine sand from the top of Unit 7 (advance phase glaciolacustrine, glacial Lake Mathews); **e)** Diamict interpreted to be till (upper Unit 9); **f)** Medium sand (base of unit 10); **g)** Contact (dotted line) between pebble- to cobble-gravel (arrows) and saturated medium sand (base of Unit 10); **h)** Laminated silty medium glaciolacustrine sand from Unit 10 (glacial Lake Peace); and **i)** Massive to weakly laminated glaciolacustrine silt and clay from the top of Unit 10 (glacial Lake Peace).

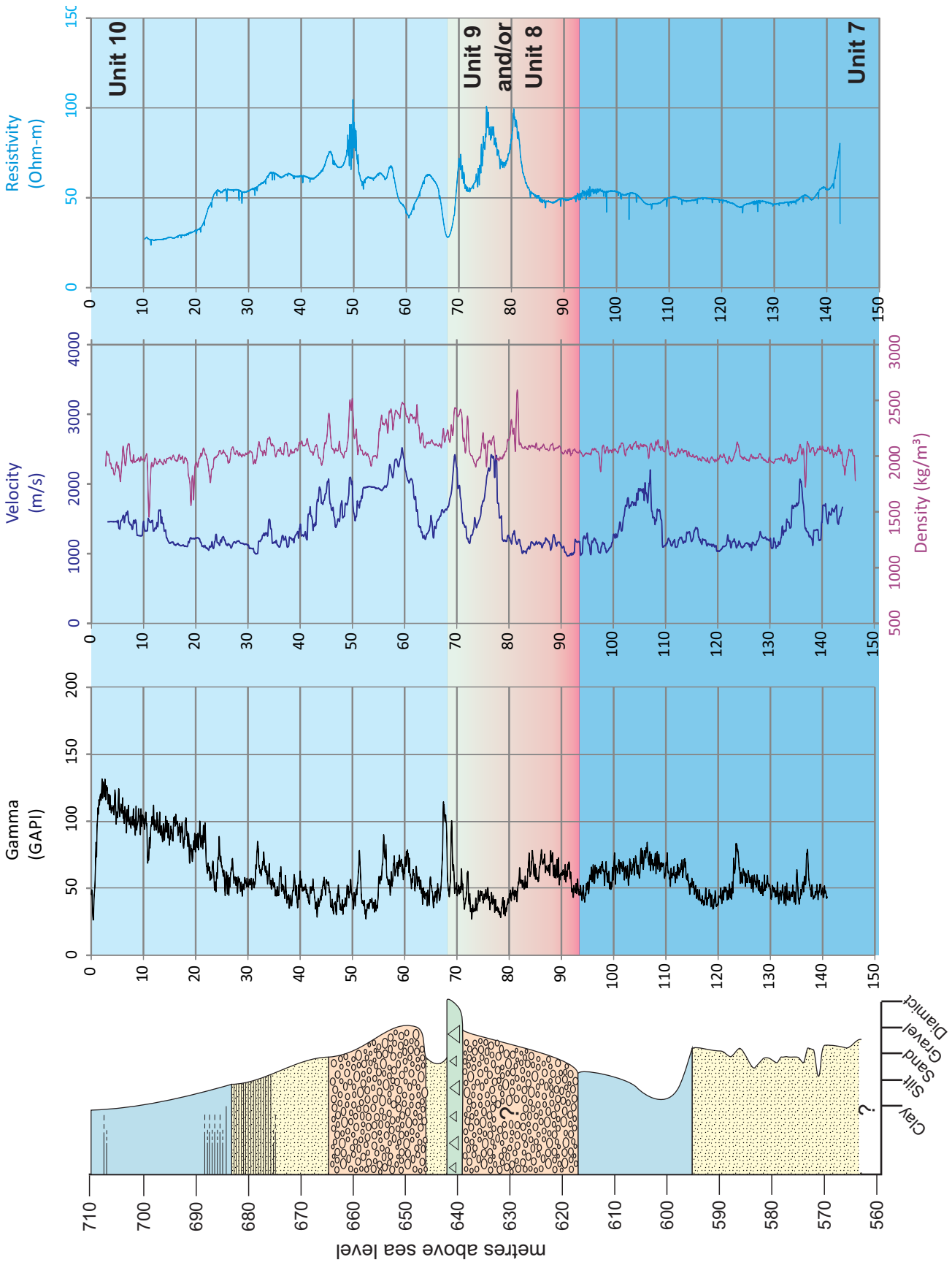

Fig. 9. Lithology log from borehole GB15-2 with gamma ray, sonic, and resistivity logs.

the lithologic data (Fig. 9), but show more within-unit variation than the logs from GB 15-1. The borehole did not intersect bedrock, and the well terminates in Unit 7. The average gamma value of Unit 7 is 55 API (Table 2). Gamma values increase upwards from the base of the borehole from about 45 to 59 API, with a small spike (maximum value of 83 API) at 587 m asl. Gamma values are lower between 587 and 595 m asl, averaging 45 API. The gamma response over the remainder of Unit 7 (595 to 615 m asl) initially increases to 70 API before decreasing over 20 m to about 30 API. The interval interpreted to be a mixture of units 8 and 9 consists of three distinct zones with an average gamma response of 52 API (Table 2). The lower zone (615 and 630 m asl) has an average gamma value of 61 API, the middle zone (630 to 639 m asl) averages 42 API, and the upper zone, which correlates with a diamict bed (639 to 641) averages 58 API. At this location, the unit fines upwards from gravel to silt and clay. The gamma response is generally consistent with the lithologic data, increasing upwards from about 50 to 130 API.

The average velocity at the base of units 9 and/or 8 and Unit 7 is about 1100 m/s. Between 100 and 110 m depth, the average velocity is about 1750 m/s in an interval interpreted to be fine grained. A slight increase in the gamma log suggests that the velocity increase may indicate a clay-rich horizon at this interval. The average velocity of Unit 10 is between 1500 m/s and 1600 m/s, although excursions are near the top of units 9 and/or 8, and at the base of Unit 10. Density varies little over the entire length of the log. The average density is about 2000 kg/m^3 with only minor variations in units 9 and/or 8 and at the bottom of Unit 10. Potential reflections are near 60 m, at the base of a gravel unit (units 9 and/or 8; Fig 9), near 80 m in this mapped gravel unit (although the gamma log and resistivity logs suggest the lower section of these units may not be gravel), and at the top of the clay unit at 100 m.

Resistivity is consistently near 50 Ohm-m through Unit 7, and the base of units 9 and/or 8. Between 82 and 70 m below surface is a marked increase in resistivity to an average of 72 Ohm-m. This increase corresponds to the middle gamma zone in Unit 9 and/or 8 and may represent a potential aquifer. Average resistivity values for Unit 10 (between 70 and 23 m below surface) are generally higher than Unit 7, averaging 58 ohm-m before dropping sharply to an average of 30 Ohm-m.

3.2.3 GB15-3

Borehole GB 15-3 is on the west side of the 273 Road (also known as Berg Road), 0.5 km north of the 208 Road (Fig. 1). The well was drilled on the north flank of the paleovalley to a depth of 69 m (631 m asl), and intersected bedrock at a depth of 53.6 m (646 m asl). The bedrock, which typically shatters during sonic drilling, is laminated mudstone (Fig. 10a). The bedrock-Quaternary sediment contact was heavily disturbed by the drilling but may be a zone of breccia. Silty to silty-clay diamict (Figs. 10b-c) overlies bedrock and is interpreted to be Late Wisconsinan subglacial till (Unit 9; Hickin, 2013). The till is overlain by poorly sorted pebble gravel that fines upward to massive and laminated or thinly bedded medium sand. The sand is overlain by laminated fine sand to massive silt with rare diamict beds. The top of the succession is massive to weakly laminated silt and clay (Fig. 10d). These sediments are interpreted to have been deposited in retreat phase glacial Lake Peace and are assigned to Unit 10.

The gamma response in bedrock from GB 15-3 is generally consistent, averaging 113 API (Fig. 11; Table 2). However, close to the base of the log is a narrow (about 1 m) excursion that decreases to 53 API. Above bedrock, the gamma response decreases abruptly from 136 to 78 API over 2 m. This decrease may reflect a brecciated bedrock-unit 9 contact. The gamma response in Unit 9 averages 79 API but can be separated in to a lower zone (648 to 654 m asl) with an average of 89 API, and an upper zone (654 to about 662 m asl) that averages 58 API. Between units 9 and 10 the gamma response remains unchanged. The gamma response in the lower 10 m of Unit 10 fluctuates near 51 API. Above this zone, the gamma response increases from 51 API at the bottom, to 130 API at the top, reflecting the general fining-upwards succession common in Unit 10.

The average velocity in bedrock is approximately 2650 m/s, although it is variable and ranges from 2160 to 3460 m/s. At the bedrock-Unit 9 contact there is a velocity spike (maximum value of 2950 m/s) (647 to 650 m asl); above this, the velocity stabilizes to about 1950 m/s. The transition between units 9 and 10 is marked by a velocity decrease from about 1700 to 1350 m/s. The lower 15 m of Unit 10 has a relatively consistent velocity around 1550 m/s. The top of Unit 10 show a sharp increase to an average of 1650 m/s.

The density response does not match well with the lithologic boundaries (Fig 11). The average density of bedrock is about 2240 kg/m^3, but decreases from 2550 kg/m^3 at the base of the logged section upwards to about 2000 kg/m^3 near the bedrock-sediment contact. Density increases in the possible breccia zone to about 2400 kg/m^3 before decreasing across

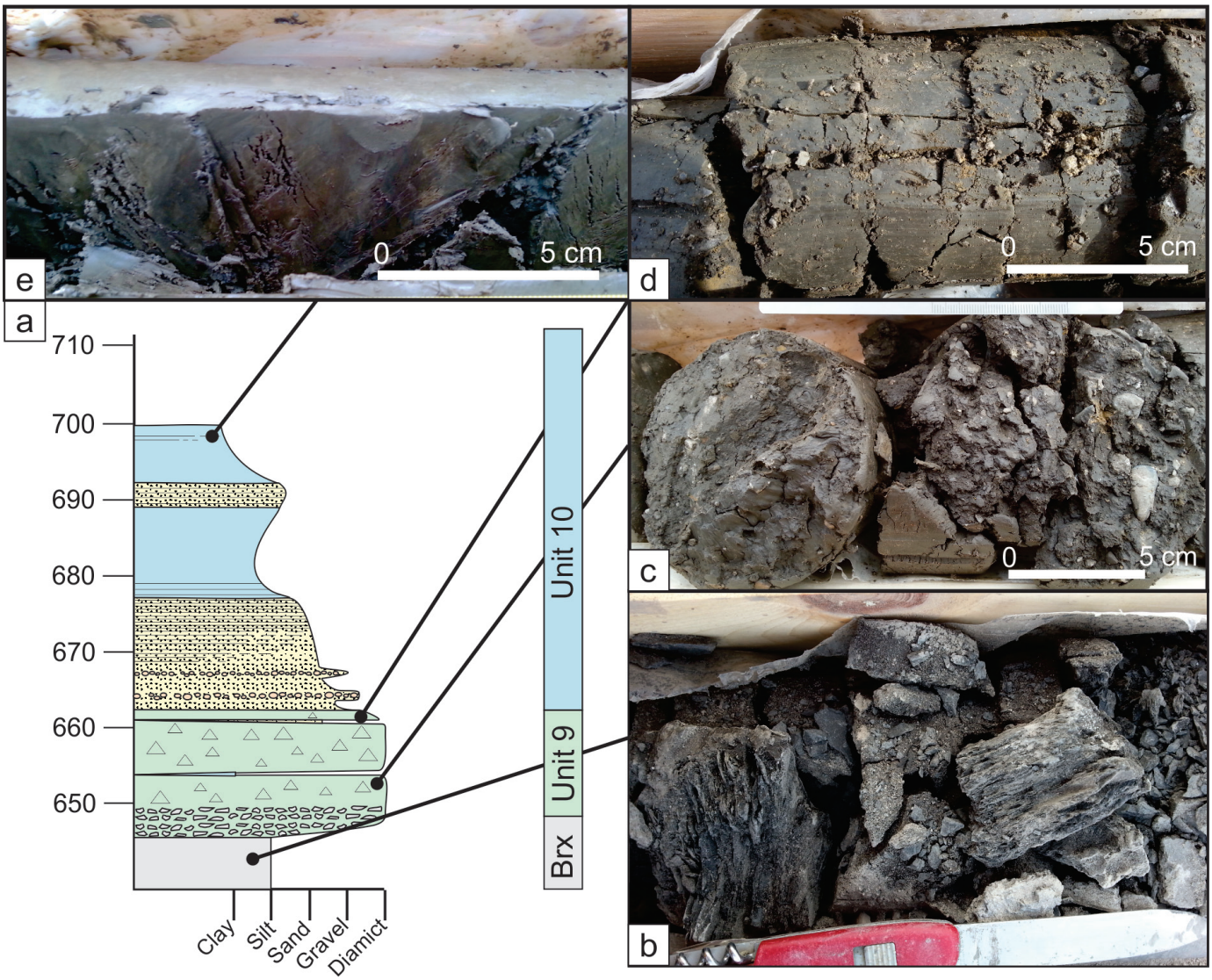

Fig. 10. Borehole GB15-3 (see Fig. 1 for location). **a)** Lithology log; **b)** Bedrock (shattering a result of sonic drilling); **c)** Diamict interpreted to be till (lower Unit 9); **d)** Diamict interpreted to be till (upper Unit 9); and **e)** Massive to poorly laminated retreat phase glaciolacustrine silt and clay.

a short interval to about 1800 kg/m^3 at the base of Unit 9. The remainder of Unit 9 averages 1970 kg/m^3. The contact between Unit 9 and Unit 10 is marked by a density drop from 1940 to 1480 kg/m^3. Unit 10 has an average density 1740 kg/m^3 but has five zones with average densities of 1610 kg/m^3 (662 to 667 m asl), 1780 kg/m^3 (667 to 675 m asl), 1575 kg/m^3 (675 to 680 m asl), 1940 kg/m^3 (680 to 692 m asl), and 1100 kg/m^3 (692 to 695 m asl). Based on the velocity and density data, a seismic reflection may be expected near the bedrock-sediment interface.

Resistivity only crudely reflects lithology. The average resistivity of bedrock is 20 Ohm-m. Resistivity averages 40 Ohm-m in Unit 9, increasing from around 20 Ohm-m at the bedrock-sediment interface to a maximum value of 75 Ohm-m at the contact between units 9 and 10. Unit 10 displays three distinct resistivity zones. The lower zone (665 to 675 m asl) has an average resistivity of 45 Ohm-m. The middle zone (675 to 681 m asl), with an average resistivity of 70 Ohm-m, may be a potential aquifer. The upper zone has an average resistivity of 28 Ohm-m.

3.2.4. GB15-4

Borehole GB 15-4 is on the east side of the 269 Road, 2.4 km south of the 208 Road (Fig. 1). The well was drilled on the south flank of the paleovalley to a depth of 70.7 m (652 m asl) and intersected shale bedrock (Fig. 12a, b) at a depth of 69.1 m (654 m asl). The contact between bedrock and the overlying Quaternary sediments is marked by a 3 m-thick, gravelly, stratified diamict consisting of rounded to subrounded shale fragments.

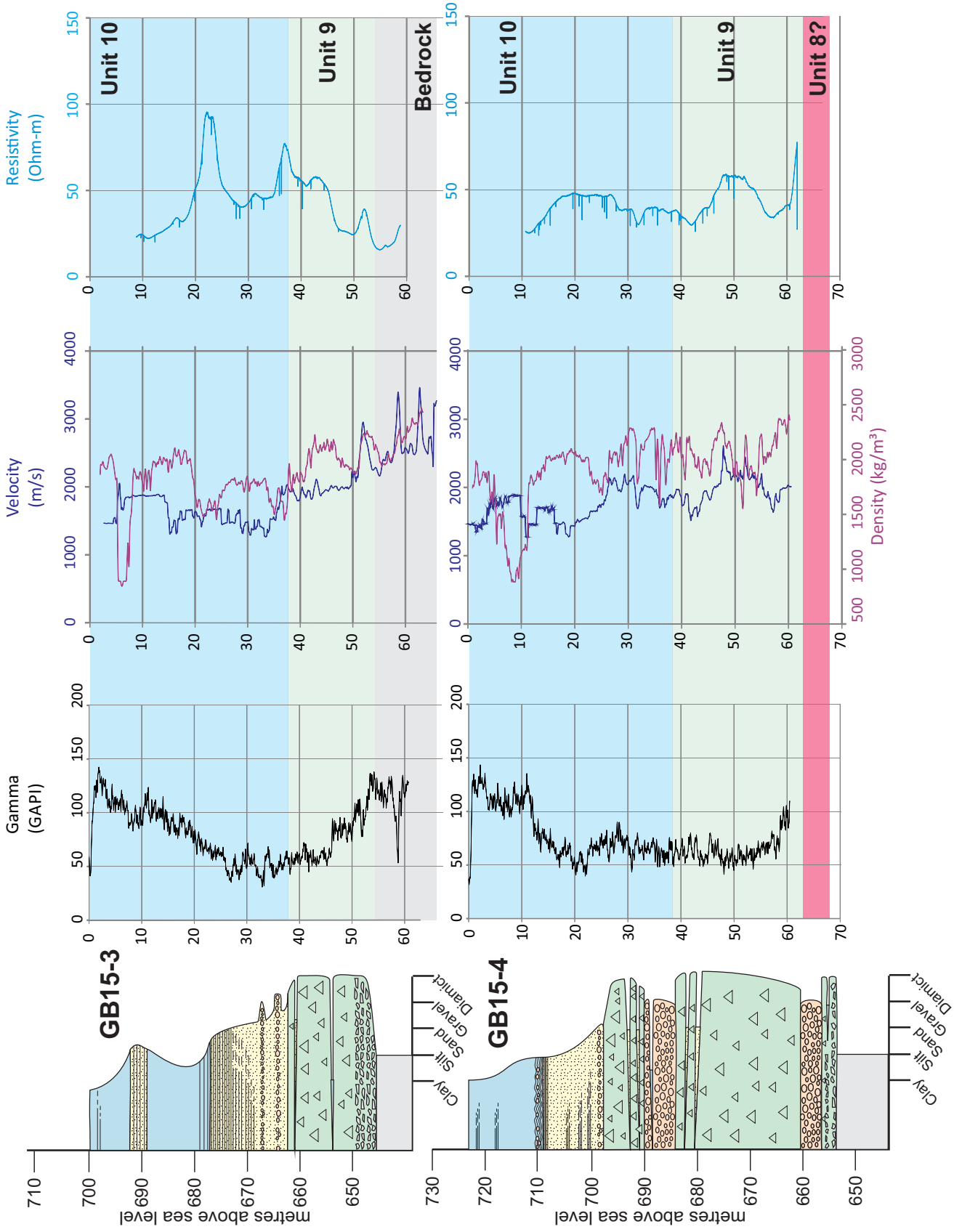

Fig.11. Lithology log from borehole GB15-3 (above) and GB15-4 (below) with gamma ray, sonic, and resistivity logs.

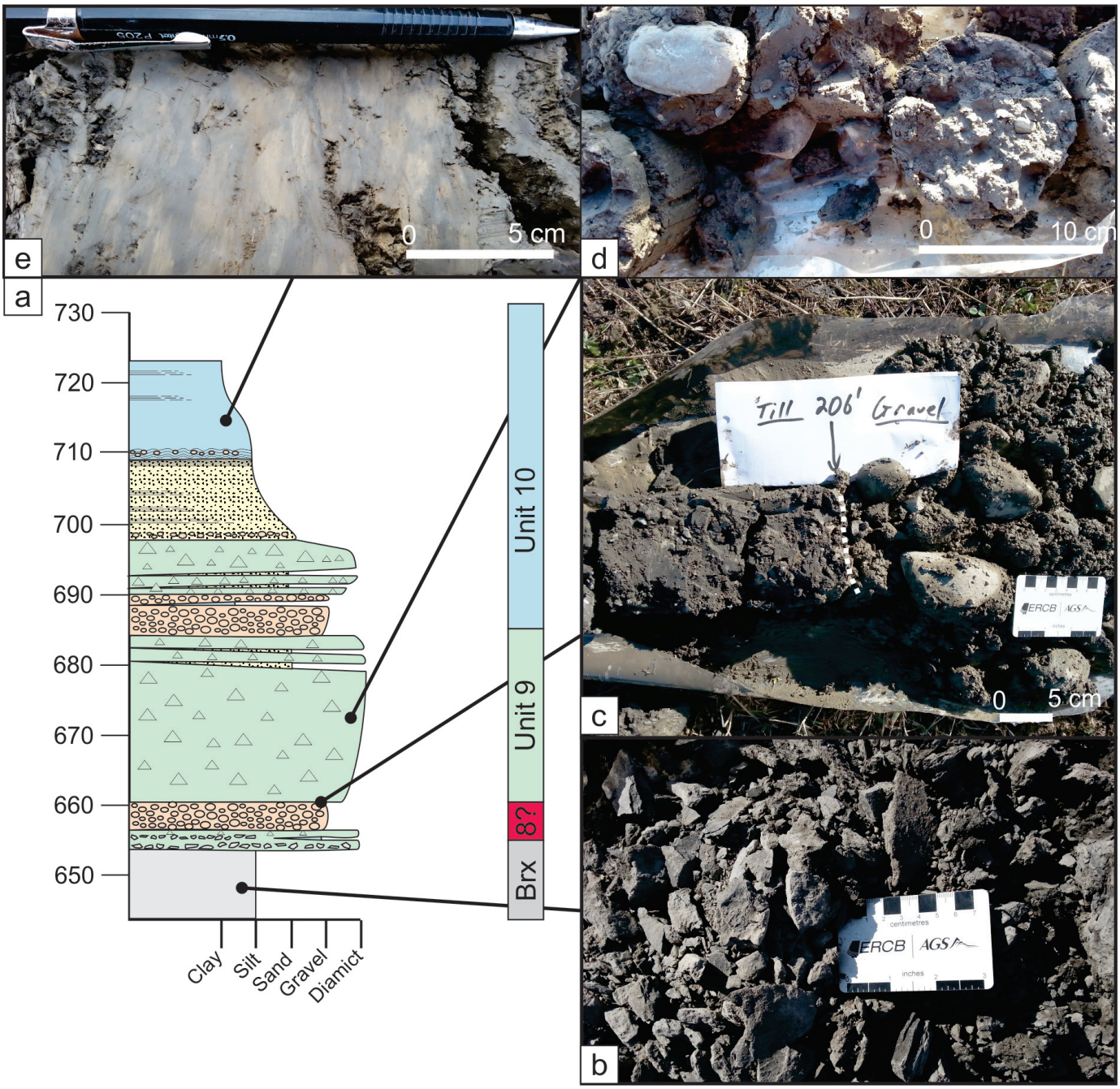

Fig. 12. Borehole GB15-4 (see Fig. 1 for location). **a)** Lithology log; **b)** Bedrock (shattering the result of sonic drilling); **c)** Contact between till and interbedded pebble- to cobble gravel (Unit 9); **d)** Diamict interpreted to be till (Unit 9); and **e)** Mottled, laminated (deformed?) retreat phase glaciolacustrine silt and clay (Unit 10).

The depositional environment is unclear, but this unit may indicate locally sourced debris flow deposits, brecciated bedrock, or glacially-tectonized gouge. Pebble gravel (4 m thick) containing sedimentary and carbonate clasts, some of which are striated, overlies the shale-clast bearing stratified diamict. A 20 m-thick diamict with a sharp lower contact overlies the pebble gravel (Fig. 12c). This diamict is dense and contains striated and faceted clasts, and is therefore interpreted to be subglacial till (Fig. 12c) correlative with Unit 9. The till is overlain by a fining-upwards succession consisting of poorly sorted gravel and diamict that grade upwards to pebbly sand, silty sand, and ultimately to clay. This succession is assigned to Unit 10, retreat phase glaciolacustrine deposits of glacial Lake Peace.

Little variation in the geophysical logs from GB 15-4 can be attributed to lithology alone (Fig. 11). Logs are

restricted to units 9 and 10 because the lowest portion of the well was constructed as a functioning water well and the base was screened for collecting water. The gamma response is consistent through units 9 and the lower 17 m of Unit 10, and the contact between units 9 and 10 is not readily apparent. Through this interval the gamma log averages 63 API. Between 701 and 710 m asl the gamma values increase from 45 to 84 API. Above this, the gamma response is consistent with minor fluctuations about an average of 114 API.

The velocity of Unit 9 increases from about 1700 m/s to a maximum of 2125 m/s at 675 m asl before decreasing to about 1570 m/s. The average velocity of Unit 9 is 1971 m/s. Although Unit 10 has an average velocity of 1715 m/s, it can be further divided into three velocity zones. The lower zone (685-698 m asl) has an average velocity of 1940 m/s. The middle zone (698 to 713 m asl) has an average velocity of 1590 m/s. The upper zone (713-723 m asl) has an average velocity of 1660 m/s.

The density log is consistent through Unit 9 and the lower 11 m of Unit 10, and remains constant across the contact between the two units. Through this interval, density fluctuates from between 1700 and 2425 kg/m^3 (average of 2100 kg/m^3). Between 698 m asl and 700 m asl, density decreases to an average of 1810 kg/m^3. Above this interval, density increases to an average of 1970 kg/m^3 between 700 and 711 m asl. Between 711 and 718 m asl, density drops sharply to an average of 1165 kg/m^3 before increasing to an average of 1800 kg/m^3 at the top of the logged section. Based on these two logs, shallow subsurface seismic reflections are unexpected.

The average resistivity of Unit 9 is 43 Ohm-m. However, resistivity values at the top and bottom of Unit 9 are about 35 Ohm-m. The central portion of the unit displays elevated values (to 57 Ohm-m). The resistivity of Unit 10 is generally consistent (average, 40 Ohm-m); in the upper 4 m, values decrease slightly to about 25 Ohm-m. The resistivity data suggest limited potential for aquifers in units 9 and 10, but the well successfully produced water in the basal gravel, which may be part of Unit 9 (Fig. 11).

3.2.5. GB15-5

Borehole GB 15-5 is southwest of the intersection of the 271 and 208 roads (Fig. 1). The well was drilled to 118.0 m (586 m asl) and did not intersect bedrock (Fig. 13). The base of the cored section consists of wet, massive and laminated medium sand (Fig. 13a) with rare dropstones (Fig. 13b) that generally fines upwards to laminated silt and clay. Intercalated in the sand, are silt and clay and rare poorly sorted pebble gravel horizons (e.g., between 612-613 m asl and 630-634 m asl; Fig. 13c). This part of the succession is interpreted to have been deposited in a proglacial lake, probably the advance phase (Unit 7; glacial Lake Mathews. Dense, silty and sandy diamict beds (Fig. 13d), about 2 m thick, occur in the silt and clay at 644 m asl and 656 m asl (Fig. 13e). These diamicts are interpreted to be till, but could be glacigenic debris flow deposits, consequently the thickness of Unit 9 is ambiguous. Nonetheless, at least the upper part of this succession is assigned to Unit 9 and is interpreted to be part of the Late Wisconsinan glacial complex. Immediately above the upper diamict is 4 m of silt, clay, and very fine sand. This coarsens upwards to medium sand with pebble gravel beds (Fig. 13f). The remainder of the section fines upwards from massive very fine sand to weakly horizontally bedded and laminated silt and clay with rare pebbles. This part of the section is interpreted to have been deposited into the retreat phase of a proglacial lake (Unit 10; glacial Lake Peace).

Geophysical logs from GB 15-5 correlate well with the lithologic data (Fig. 14). The gamma response in Unit 7 consistently increases from 50 API at 590 m asl to 95 API at 629 m asl, reflecting a general fining upwards in grain size. Coincident with a gravel horizon at 630 m asl, gamma drops markedly, to an average of 57 API (Fig. 14). Above this, the gamma response fluctuates, but generally increases to 110 API at 645 m asl. The inferred contact between Unit 7 and Unit 9 and/or 8 lacks a significant gamma response. The boundary between these units is arbitrary and simply reflects the presence of diamict (probably till) beds. Unit 9 and/or 8 has two gamma zones, the lower (between 645 and 655 m asl) displays an average gamma value of 98 API and the upper (between 655 and 659 m asl) has an average gamma value of 78 API. The average gamma response for the lower 4 m of Unit 10 is 80 API, above which the gamma response decreases sharply to an average of 49 API (between 662 and 675 m asl). Between 675 and 693 m asl, the gamma response is consistent and averages 92 API. From 693 m asl to the top of the logged section, the gamma values increase (96 to 130 API), reflecting a fining upwards from predominantly sand to predominantly silt and clay.

The velocity of Unit 7 varies, but generally decreases from 3300 at the base of the logged section to about to 2000 m/s at the inferred contact between Unit 7 and Unit 9 and/or 8 (Fig. 14). In the lower portion of Unit 9 and/or 8, between 644 and 652 m asl, velocity decreases to an average of about 1600 m/s. The top of Unit 9 and/or

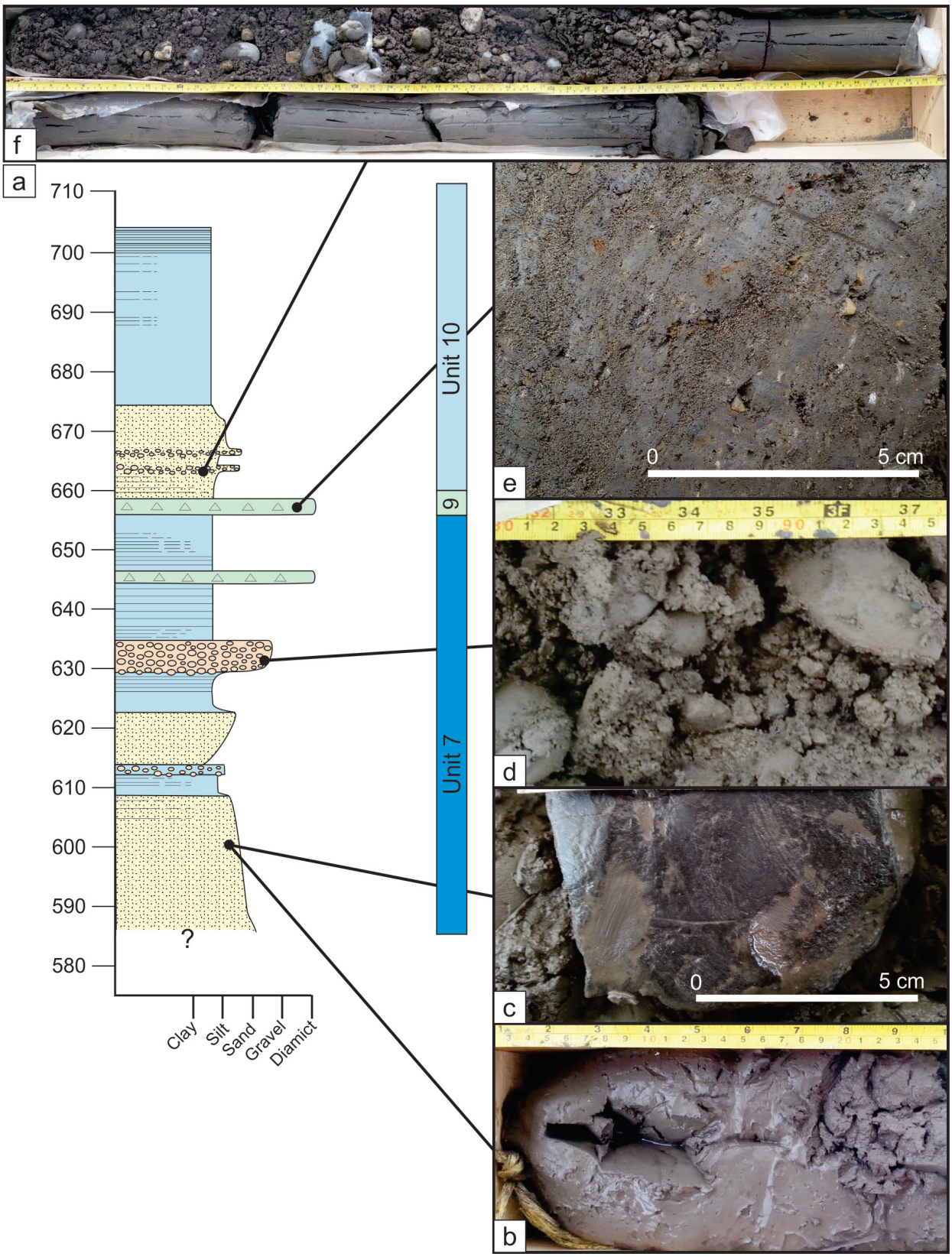

Fig. 13. Borehole GB15-5 l (see Fig. 1 for location): **a)** Lithology log; **b)** Silty-fine sand, advance phase glaciolacustrine (Unit 7); **c)** Isolated striated dropstone from Unit 7; **d)** Interbed of silty sandy pebble- to cobble-gravel (Unit 7); **e)** Interbed of diamict interpreted to be till (Unit 9); and **f)** Pebble gravel over silt and sand from retreat phase glaciolacustrine deposits of glacial Lake Peace (Unit 10).

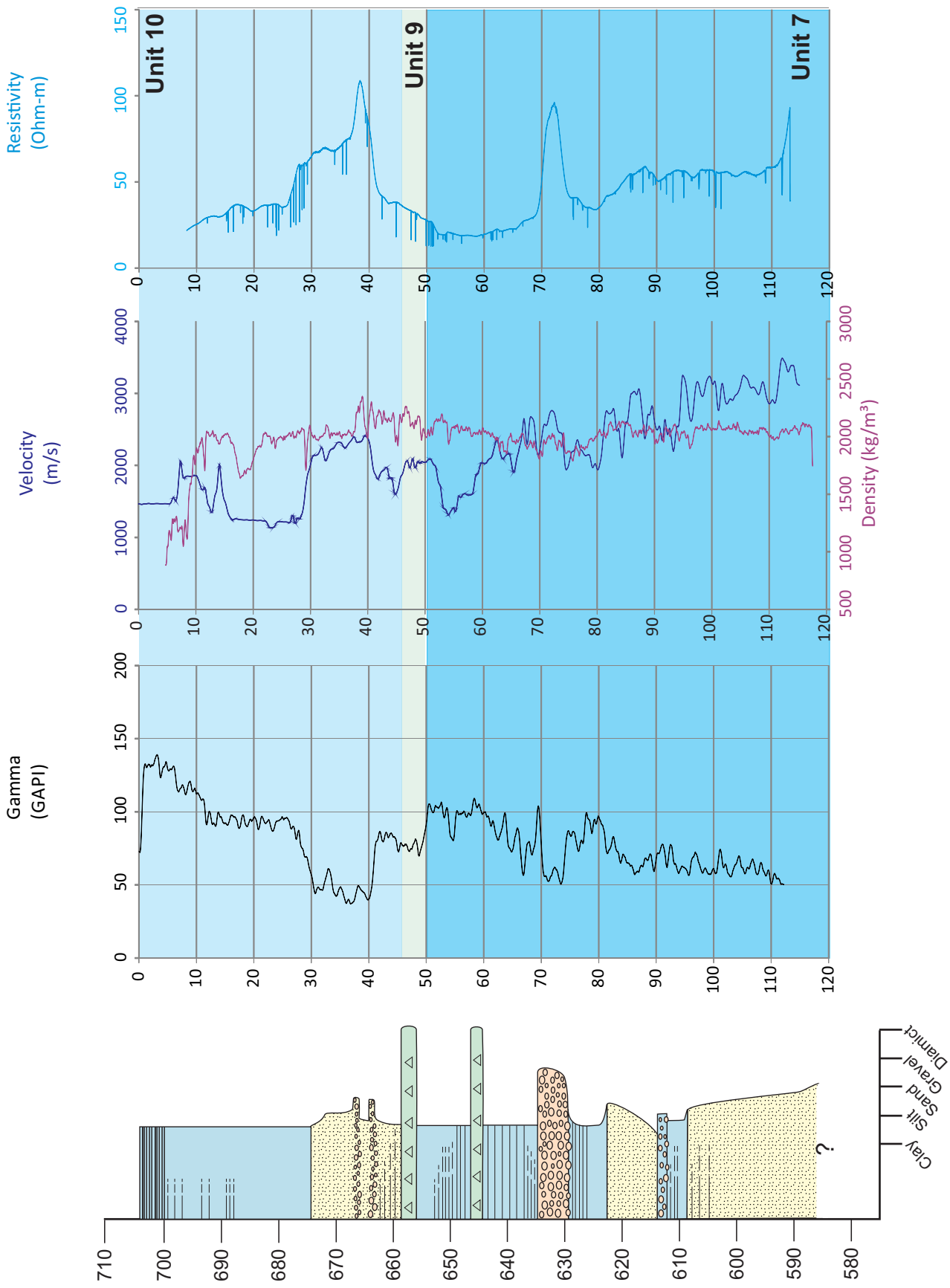

Fig. 14. Lithology log from borehole GB15-5 with gamma ray, sonic, and resistivity logs.

8 (between 652 and 659 m asl) has an average velocity of 2050 m/s. The base of Unit 10 (lower 4 m) averages 1850 m/s before sharply increasing to an average velocity of 2215 m/s between 662 and 674 m asl. Above this interval, velocity sharply decreases to an average of 1230 m/s between 674 and 688 m asl. The average velocity of the top of Unit 10 is 1685 m/s.

The density log displays little variation, with only minor fluctuations between 586 m asl and 683. Through this interval the average density is 2035 kg/m^3, and major density changes coincident with lithologic boundaries are lacking. Between 683 and 689 m asl, the average density drops to 1810 kg/m^3 before returning to an average density of about 2030 kg/m^3. Based on the above one might expect a seismic refection at the top of the Unit 10 gravels and at the interface between units 9 and 7.

The average resistivity is 50 Ohm-m between 590 and 620 m asl and drops slightly to 35 Ohm-m between 620 and 629 m asl. A significant resistivity spike (to 87 Ohm-m) correlates with a gravel bed between 629 and 635 m asl. This interval is an excellent aquifer target. The top of Unit 7, all of unit 9 and/or 8, and the base of Unit 10 are between 635 and 662 m asl and have consistently low average resistivity of 22 Ohm-m. Above this is another resistivity spike (between 662 and 678 m asl) with an maximum resistivity of 98 Ohm-m that correlates with a sandy interval, a gamma low (49 API) and a velocity high (2215 m/s). This interval is also an excellent aquifer target. Between 678 m asl and the top of the logged section, resistivity values decline to an average of 28 Ohm-m.

3.3. Shallow seismic reflection methods

3.3.1. Data acquisition

The seismic source is an IVI (Industrial Vehicles International, Inc) "Minivib 1" vibrator mounted on a "minibuggy" (Fig. 15a). This source vibrates a 140 kg mass in either vertical or horizontal mode, and allows the operator to program the sweep through a range of frequencies between 10 and 550 Hz. The drive amplitudes

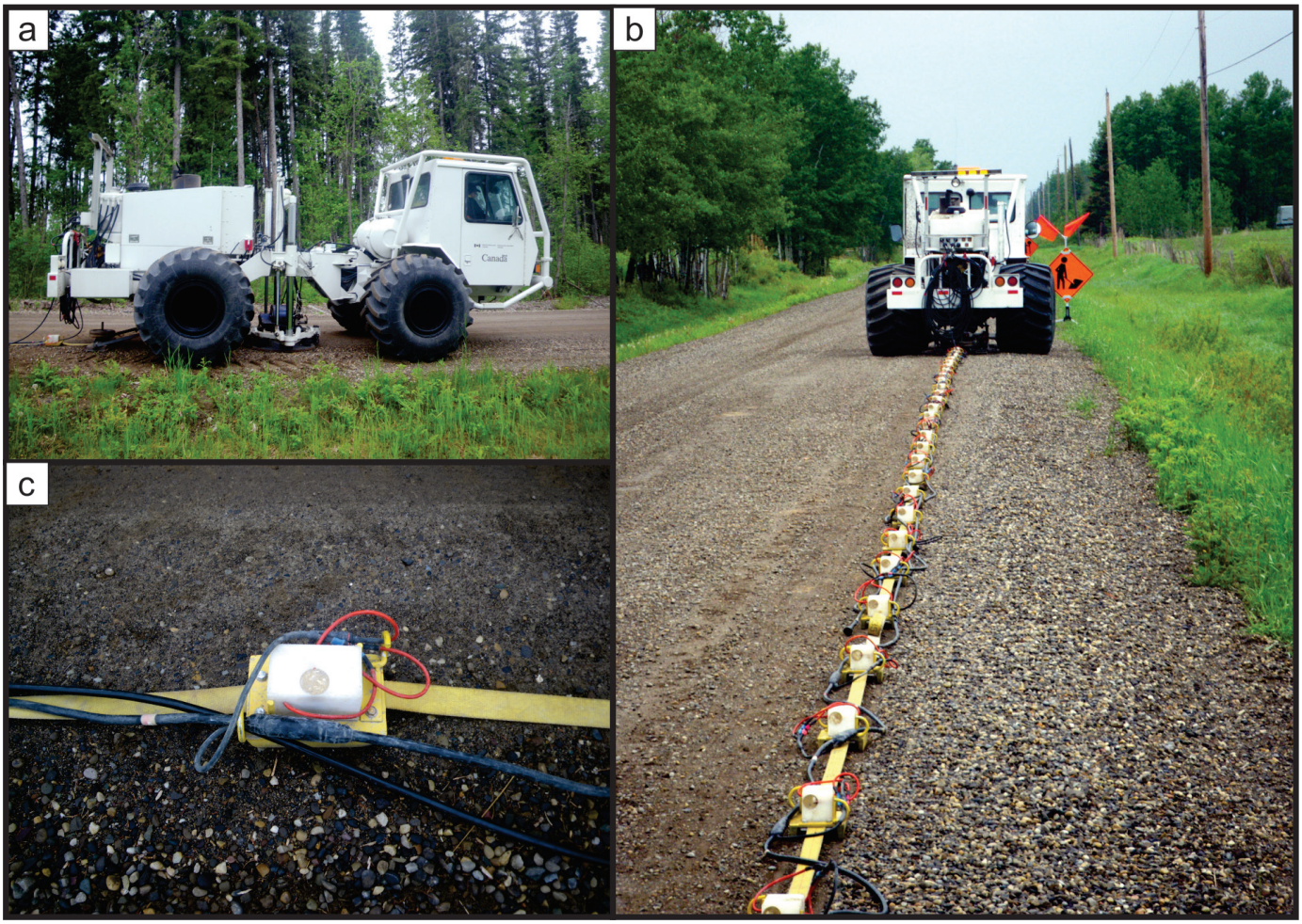

Fig. 15. a) The Geological Survey of Canada's mini-vibe source for the shallow seismic survey; **b)** The land streamer is towed behind the mini-vibe source enabling rapid data collection; and **c**) The three component geophones mounted on a metal sled.

are set at 70% of the vibrator's possible motion. A high-precision odometer is linked to a small readout screen mounted in the cab, allowing the operator to move quickly and accurately to the next shotpoint while the seismograph is saving data. Data were recorded using six 24-channel Geometrics Geode engineering seismographs in the cab of the Minivib. Uncorrelated records are recorded to allow prewhitening of the data, necessary to ensure stability of the deconvolution filter; careful choice of the correlating function is the first step in processing the data. For this survey, the Minivib was operated in the inline horizontal vibrating mode using a 7 second linear sweep from 10-280 Hz with a nonlinear sweep DB/Oct-2.

The Geological Survey of Canada's landstreamer is designed for use along paved or gravel roads, and is built with 72, 3 kg metal sleds connected using wire or low-stretch rope (Fig. 15b). The number of receivers and the receiver spacing can be varied depending on the near-surface velocities and the targeted depths of observation. For these surveys the landstreamer array consisted of 48 sleds spaced 1.5 m apart. Each sled was equipped with a 3-component (3-C) geophone unit constructed in-house with 30 Hz omni-directional geophone elements oriented in three directions: one vertical and two horizontal, in-line and cross-line (Fig. 15c). Three-component data were acquired with shotpoints every 4.5 m along the survey lines.

Using the Minivib/landstreamer system described above, approximately 1000 records or about 4.5 line-km of data are typically recorded per day. An example field record (144 channels) is shown in Figure 16. Channels 1-48 are the vertical (V) geophones; 49-96 the in-line horizontal (H1) geophones; and channels 97-143 the cross-line or transverse horizontal (H2) geophones.

3.3.2. Shallow seismic data processing

The reflection data can be processed to provide both P-wave (compressional-wave) and S-wave (shear-wave) sections even though the mass was vibrated in one orientation (Pugin et al., 2009). In this case, P-wave sections are derived from processing the first 500 milliseconds (after correlation) of data acquired on the vertical geophones, whereas S-wave sections are produced from 2 sec of the in-line H1 component of recorded data. Processing sequences are similar, although different filters and stacking velocities are required for the two data sets (Table 3).

3.4. Shallow seismic reflection results

The survey included 9 lines totaling about 50 km (see Fig. 1 for location and Appendix C for the complete suite of profiles). The vibroseis survey data were generally of poor to moderate quality. Reflections in the early portion of the record (0-0.2 seconds) were generally strong, although deeper reflections were more difficult to resolve. Because initial mapping indicated that depth to bedrock should be less than about 100 m, we selected geophone a spacing to focus on shallow levels. However, the survey results suggest that bedrock in the deepest part of the paleovalley may be 250-350 m deep. As a result, the reflector that represents bedrock could only be identified in a few sections.

Water well records, warehoused by the British Columbia Ministry of Environment and obtained using the Groundwater Information Network, include lithologic summaries and depths to water-bearing units as reported by drillers. Although some drillers may be familiar with the local stratigraphy, observations made by different operators are typically of variable quality, and well logs from one well to another are commonly inconsistent, which limits confidence in the lithologic data.

The average velocity from ground surface to the reflection event can be determined by analyzing the hyperbolic reflection events in the common midpoint (cmp) gathers (e.g., Fig. 17). These data allow the interval velocities to be established. The sediments have high S-wave average velocities (250-600 m/s) and P-wave average velocities (800-2200 m/s). Velocities from the boreholes are consistent with those from the seismic survey.

In general, the seismic data define major reflectors that bound distinct seismic facies, which can be related to the lithostratigraphic facies established by borehole data. The lowest significant reflector (e.g., Fig. 18b, c; Appendix C) is detected in profiles along the 208 Road (east end), Stucky Road (east end), 269 Road (central), and Lindsey Road (west). This reflector is generally weak, discontinuous, and typically best observed in the P-wave. Based on velocity, we tentatively interpret this reflector as the top of the bedrock surface. Unfortunately, this reflector was not intersected by drilling of the deep portions of the paleovalley. Furthermore, with the exception of the east side of the profile along Stucky Road, the reflector is not expressed near higher elevation ridges south of Highway 97 (Fig. 1) where we expected bedrock at shallow depths. It is present in the upper 30 m on the south end of the profile along 269 Road, which implies ridges to the south are bedrock controlled. Although we are confident interpreting this reflector as the bedrock surface at the south ends of the 269 Road, it remains ambiguous in the

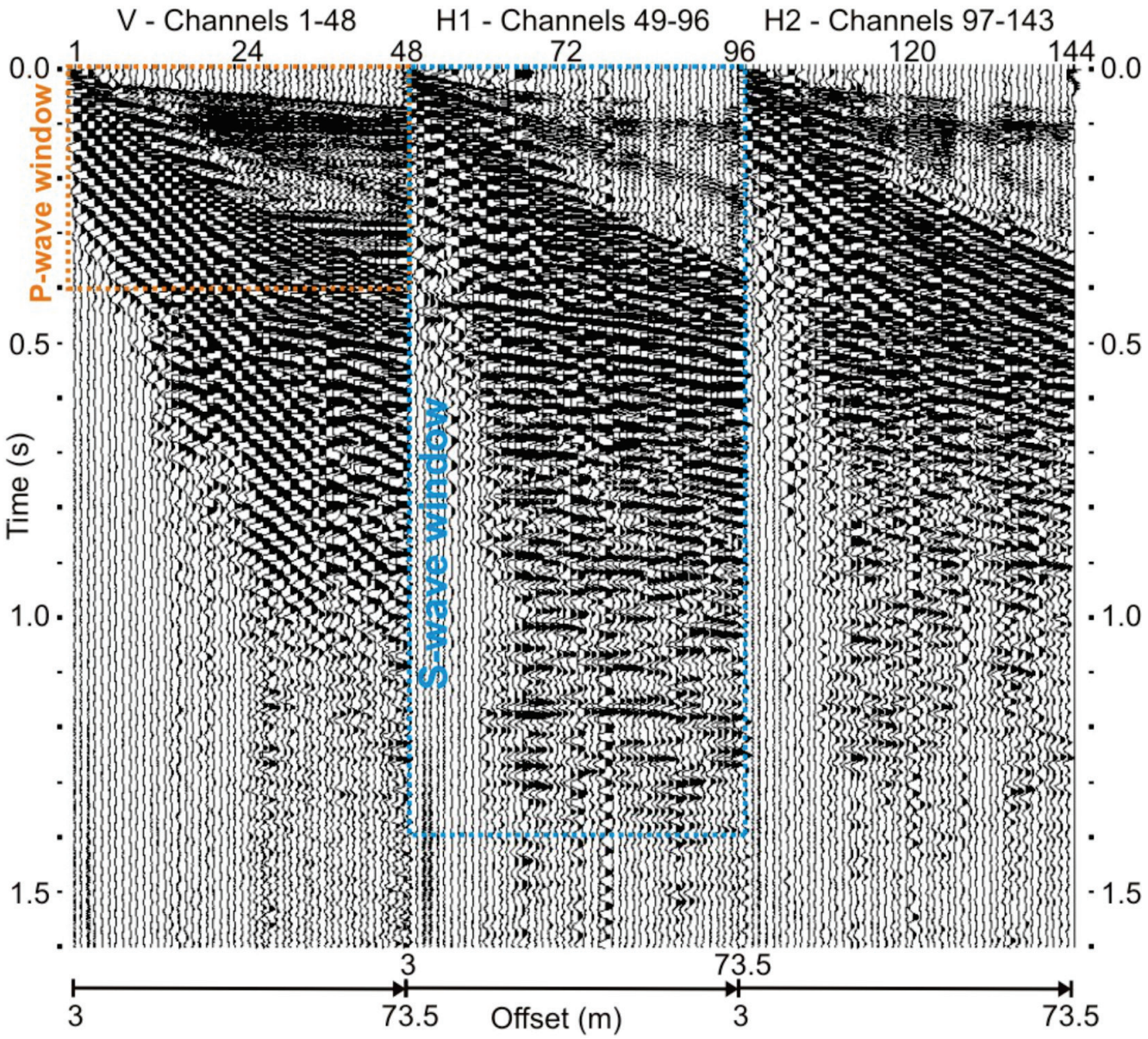

Fig. 16. Deconvolved 3-component seismic record from the Groundbirch survey (Line 208). The source was vibrated in the H1 (in-line horizontal direction). The orange rectangle outlines the P-wave reflection (P-wave reflections are best observed on the vertical component). The blue rectangle outlines the shear-wave reflection package (best seen on the H1 component only).

deepest portions of the paleovalley. Boreholes GB15-2 and GB15-5 terminated before reaching bedrock, and the reflector occurs below where drilling ceased.

An uncommon reflection (labelled "unknown"; e.g., Fig. 18b, c; Appendix C) is above the bedrock reflector on profiles along the 208, 269, and 271 roads. The reflection occurs in isolation or onlaps the bedrock reflection. Between bedrock and the unknown reflection, the P-wave seismic facies include semi-coherent (over a few hundred m) to chaotic reflections. The cause of these reflections is unclear, but the velocity and seismic facies suggest that it records unconsolidated and possibly diamict and gravel lenses (cf. Pugin et al., 1999). This zone may host, in part, units 2, 3, and/or 4 of the pre-late Wisconsinan glacial succession (Hickin, 2013); however, this interpretation remains unsubstantiated.

A uniform semi-transparent zone, >200 m thick, occurs above the "unknown" and bedrock reflections (Fig. 18b, c). Although this zone contains no coherent reflections, the interval velocity is consistent with silt and sand. Boreholes GB15-1 and GB15-2 penetrated this zone, which is equivalent to Unit 7 (advance phase glacial

Table 3. Seismic data processing.

Initial processing (all data)	
Format conversion, SEG2 to KGS SEGY	
AGC widnow of 1 second (spectral whitening)	
Pilot trace-based deconvolution	
Separation of V, H1, H2 components	
Editing of the geometry / Sort	
P-wave **V component data**	**S-wave** **V component data**
Edit-kill bad traces	Edit-kill bad traces
Frequency filter (BP 80-120-270-310 Hz)	Frequency filter (BP 25-40-90-110 Hz)
Scaling (trace normalization)	Scaling (trace normalization)
Surgical mute (air wave, surface waves)	Top mute (P-wave, surface waves)
Velocity analysis (cmp gathers: 2.25m bins)	Velocity analysis (cmp gathers: 2.25m bins)
NMO Corrections (~800-2200 m/s)	NMO Corrections (~100-400 m/s)
Stack, nominal fold: 24	Stack, nominal fold: 24
Frequency filter (BP 80-120-270-310 Hz)	Frequency filter (BP 25-40-90-110 Hz)
Correction for ground surface topography	Correction for ground surface topography
Conversion to depth (using NMO velocities)	Conversion to depth (using NMO velocities)

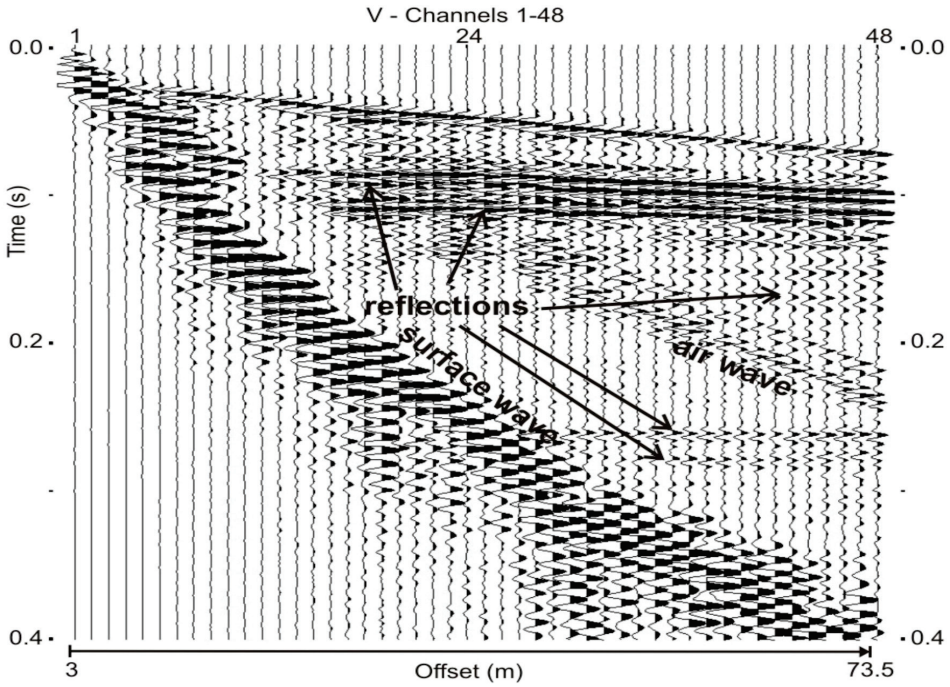

Fig. 17. Filtered (Low cut 90 Hz) P-wave vertical seismic record from the Groundbirch survey, Line 208. The source was vibrated in the H1 (in-line horizontal direction). Deep 0.28 s P-wave reflections (equivalent of the 1.2 s S-wave reflection in the H1 component indicate a thick unconsolidated deposit (see Fig. 16).

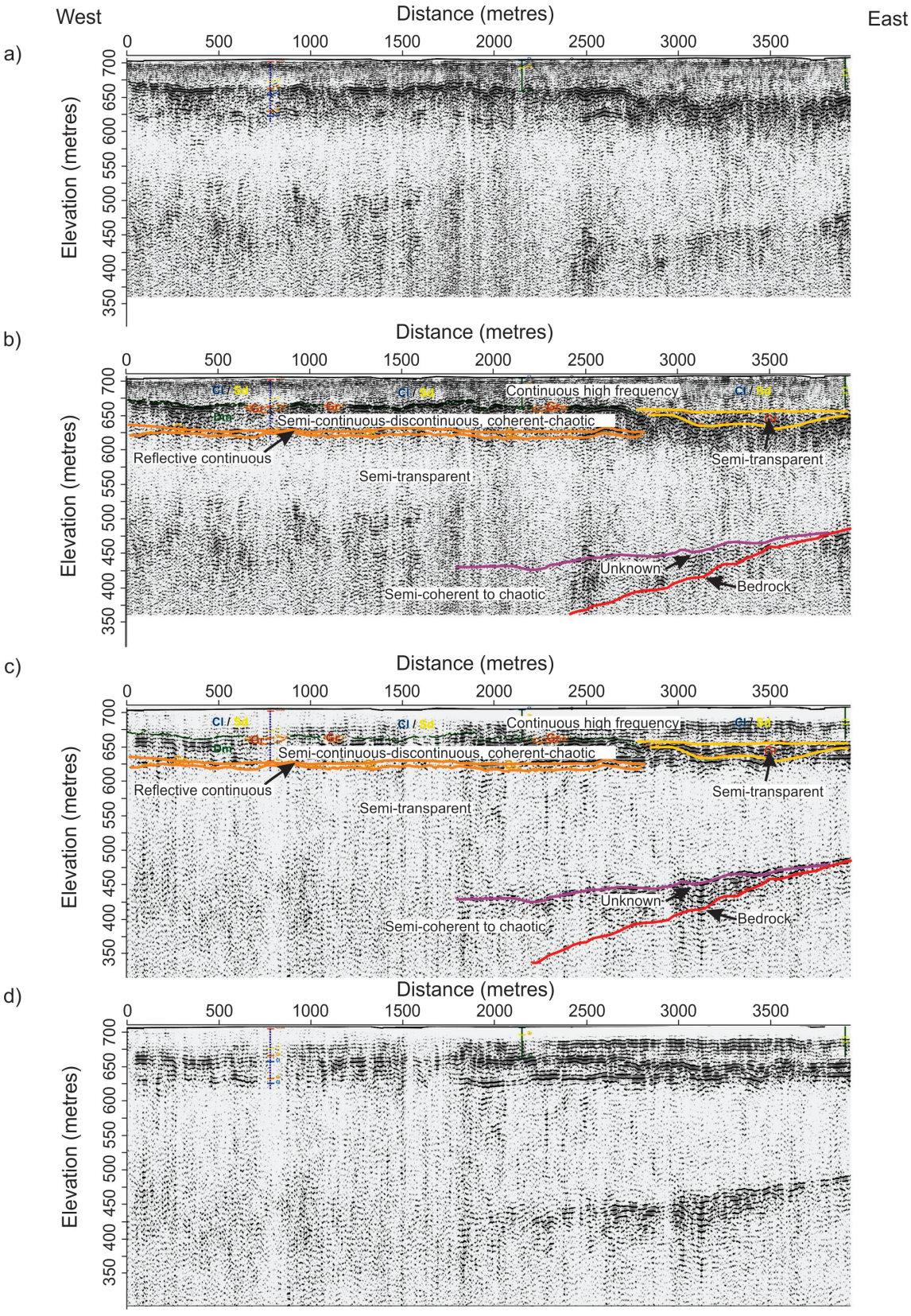

Fig. 18. Example of an S-wave and P-wave seismic section (208 Road) over the deep buried valley (full scale available in Appendix C). **a)** Raw S-wave profile; **b)** Interpreted S-wave profile; **c)** interpreted P-wave profile; **d)** raw P-wave profile.

Lake Mathews; Hickin 2013). The top of the transparent zone is typically bounded by a reflective, relatively continuous, undulating P-wave reflection. This reflection forms a narrow zone in the S-wave data, with velocities that suggest gravel. Gravel in this general stratigraphic position was intersected in GB15-2 and GB15-5 and is interpreted to represent coarse-grained beds in either the upper part of Unit 7, or gravel in units 8 or 9.

Another strong P- and S-wave reflection bounds an interval of semi-continuous to discontinuous, coherent (several hundred metres laterally) to chaotic reflections with velocities that suggest sand, gravel, and diamict (Fig 18b, c). This zone was intersected by all of the bore holes and represents Unit 9 or a combination of units 8 and/or 9.

Above this interval, a poorly developed, semi-transparent zone occurs either as a 10-20 m-thick horizon or as discontinuous zones above depressions in the lower bounding reflector (Fig. 18b, c). This seismic zone appears to fill depressions (possibly channels). Gravel was intersected above Unit 9 in boreholes GB15-1 and GB15-2, and coarse sand was intersected above Unit 9 in boreholes GB15-3, GB15-4, and GB15-5. Thus, we assign this seismic zone to the coarse-grained base of Unit 10, which marks the transition from ice-contact to glaciolacustrine sedimention.

The top of the seismic sections usually contains 50-75 m of continuous, high frequency reflections (S-wave) distinct from the underlying seismic facies. This zone is interpreted to be well-bedded silt, sand, and clay representing deposition in retreat phase glacial Lake Peace.

The profile along the 208 Road shows many of the features typical of the seismic lines from this survey and serves as an example (Fig. 18). Line 208, the most southerly east-west line (Fig. 1), is about 4 km long. All the sections shown in Figure 18 have an approximate vertical exaggeration of 2x. The uppermost section displays the uninterpreted S-wave reflection profile obtained using the H1 component data; the second section displays the same profile with picked horizons. For a better visual comparison the order is reversed with the third section showing the interpreted P-wave and the fourth section is the raw P-wave section.

What we interpret as the bedrock reflector is on the east end of the profile at 485 m asl. If correctly interpreted, it delineates a deeply buried valley, which was unknown before the seismic data were collected. This reflector implies the paleovalley has a very steep gradient of 0.13 (slope = 7.6°) and plunges to the west to a depth of >350 m. Based on the depth to bedrock recorded in borehole GB15-3, the paleovalley wall would have a slope of >20°. The reflection disappears because the geophones were spaced to optimize resolution in the upper 100 m, the total length of the landstreamer was insufficient to detect later reflections from greater depths. The unknown reflector occurs above, and onlaps the bedrock reflection to the west.

Above the unknown layer is a semi-transparent zone, about 200 m thick, with velocities that suggest a succession of fine sand and silt (Unit 7). The top of this zone is bounded by the reflective semi-continuous layer interpreted to be a coarse-grained horizon equivalent to the top of Unit 7 or a coarse-grained facies of units 9 and/or 8 (Fig. 18). This layer probably coincides with the saturated sand and gravel from boreholes GB15-2 and GB15-5. Above the gravel is a 30-40 m-thick high-velocity zone that is interpreted to be diamict. Base on boreholes GB 15-2 and GB 15-3, this unit is probably polygenetic, including glaciolacustrine sand, silt and clay, subglacial outwash sand and gravel, and till (units 9 and /or 8). The upper gravel that marks the transition from Unit 9 to 10 fills depressions and was probably deposited as channels (most likely subaqueous and/or subglacial). The top horizon is characterized by about 50 m of continuous to semi-continuous reflections up to the transparent facies and is interpreted to be a mix of sand, silt, and clay layers correlative with glaciolacustrine sediments (glacial Lake Peace).

3.5. Electromagnetic (EM) method

3.5.1. Acquisition and initial processing

We used the Geonics EM-47 time-domain electromagnetic system (Geonics, 2011). It was set up in the central sounding mode with the receiver coil (Fig. 19a) at the center of a square transmitter loop (Fig. 19b; McNeill, 1994). The transmitter controls the shape and frequency of the transmitted current. The current was fed into a 100-m square loop consisting of a single turn of insulated copper wire. A reference cable was connected between the transmitter and the Protem 47D receiver to control the timing of the transmitted waveform and the length of time the receiver voltage was measured. The plane of the high-frequency receiver coil was horizontal; hence the receiver coil measured the time derivative of the vertical component of the magnetic field (dBz/dt). Faraday's Law (Reitz and Milford, 1962) was then used to relate the time derivative to the voltage across the coil (measured in nV/Am^2 because voltage is normalized to the dipole moment of the transmitter loop).

The transmitter current approximates a square wave

Fig.19. a) EM-47 receiver coil placed in the centre of the large 100 x 100 m loop and connected to the EM-47 control console; **b)** Laying out the single turn 100x 100 m loop; and **c)** EM-47 control consol.

with a sine-wave rise time and a linear ramp at the end of the square wave when the current is turned off. The frequency of the square wave is equal to 1/T, where T is the period of the square wave pulse (in seconds). The period consists of a positive square wave of duration T/4, followed by an off time of duration T/4. This is then reversed to give a total period equal to T. The frequencies used for this survey were: Ultra High frequency (UH) = 285 Hz, Very High frequency (VH) = 75 Hz, and High frequency (H) = 30 Hz. The receiver voltage was measured in 20 time windows during the transmitter off times for each of the three frequencies. The time windows are logarithmically spaced so they are larger at longer times. The time of the window centres range from about 6.8 µs to 7 ms (UH times, 6.8 µs– 696 µs; VH times, 35 µs–2.79 ms; and H times, 88 µs– 6.98 ms, thus providing overlap between the three different frequencies).

Voltages in each of the 20 time windows were time averaged and stored in the Protem 47D console (Fig. 19c). Three sets of time-averaged voltage measurements were recorded at each of the three frequencies (UH, VH and H), providing 180 values for each sounding. The data were downloaded each day to a computer using software supplied by Geonics. This software then averaged the three sets of time-averaged voltages at each frequency to yield a data set compatible with Interpex's IX1D.v3 software (Interpex, 2006).

Sixty-five soundings were made in about 10 days. Soundings were recorded along several east-west and north-south roads (Fig. 1). The centre of the transmitter loop was 100 to 150 m away from roads and/or power lines to reduce cultural noise. Generally the centres were in open fields, but a few were in heavily wooded areas. Spacing between sounding centres was nominally 400 m, but the actual spacing depended on the location of fences and other obstacles.

3.5.2. Manipulation of the EM data using Interpex IX1D.v3

A one-dimensional (1-D) modeling and inversion software package (Interpex IX1D.v3) was used for final editing and processing of the data. The software package converted the voltage data to late-time apparent resistivity data (Spies, 1983; Spies and Eggers, 1986). These data were then edited to remove saturated voltages at early times, i.e., voltages that were above the maximum voltage of the EM system (reflects the gain setting used during data acquisition). Late-time voltages in the noise envelope were masked, i.e., the values are shown with an x, but are not used for modeling (Fig. 20). The edited late-time resistivity versus time data were then used to interpret the soundings as 1-D layered earth resistivity models. The software provides options for carrying out the modeling: 1) a smooth multi-layer model with thicknesses computed on a logarithmic scale and the resistivity of each layer calculated using inversion (for example Occam's inversion; Constable et al., 1987); 2) a layer model, with a relatively small number of layers that are inverted for thickness and resistivity and with options for fixing either resistivity values or thickness values of individual layers; and 3) an error estimation option using "equivalence analysis."

3.6. Electromagnetic (EM) results

3.6.1 Maximum depth of exploration for the EM-47

Geonics developed an empirical relationship for estimating the maximum depth of exploration for ground time-domain EM systems (personnel communication Geonics, 2015). The equation below and the graph in Figure 21 (for a current of 3 Amps) were developed based on their experience with these systems.

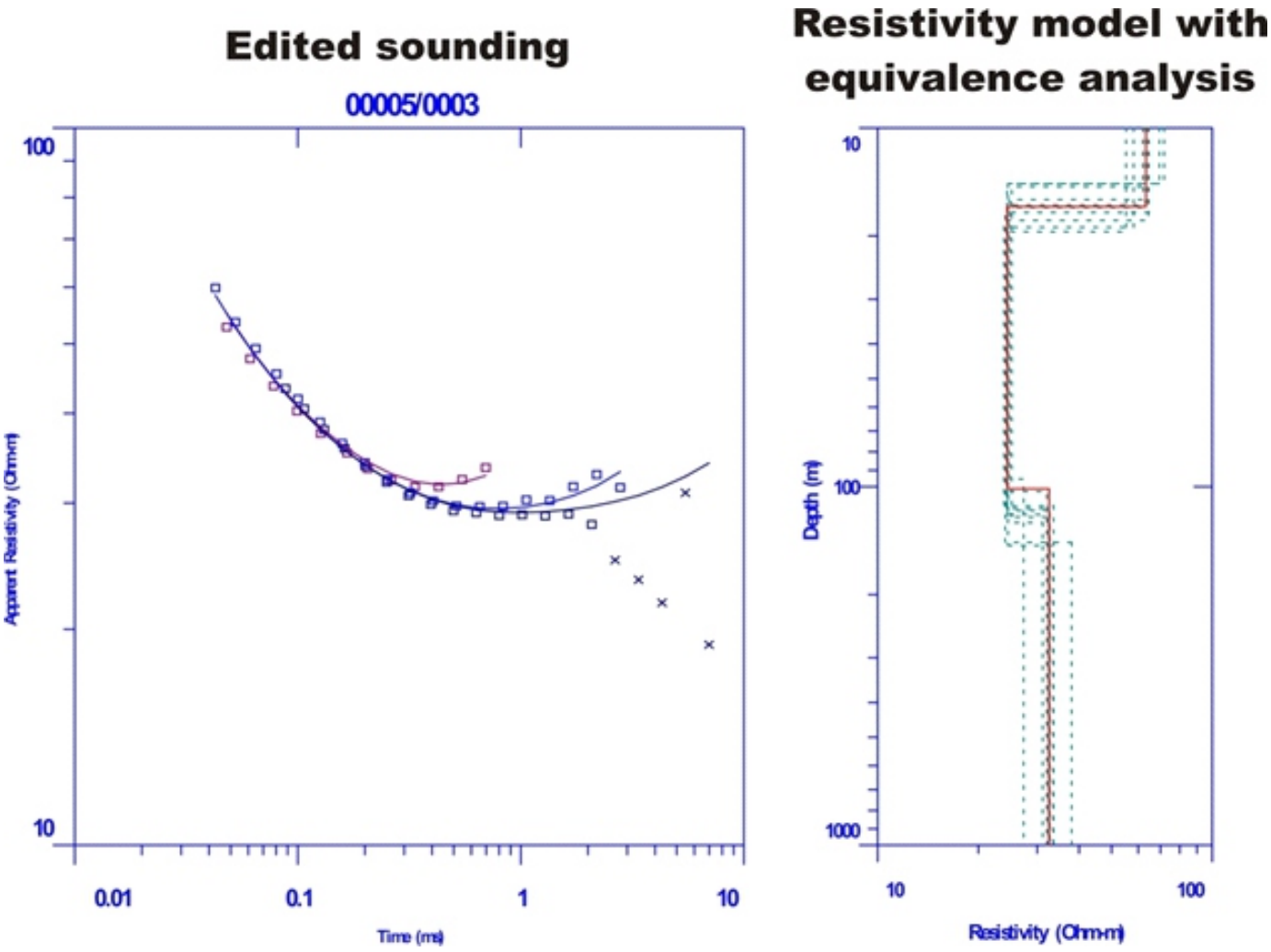

Fig. 20. Example of a typical sounding (Sounding 5 on 271 Road). **a)** Edited late-time apparent resistivity versus time; **b)** 1D resistivity inversion. The solid line is the best fit layered earth model (3 layers) and the dashed lines are 3-layer earth models with similar error of fit. The RMS error of the best fit layered earth model is 3.19 %.

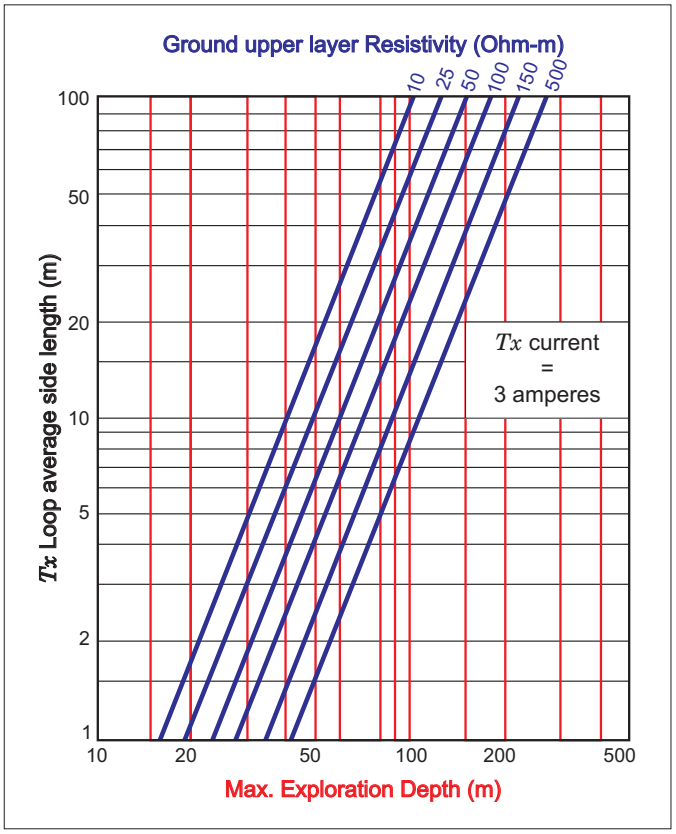

Fig. 21. PROTEM 47 exploration depth.

The maximum exploration depth (d) for a ground time-domain EM (for example the EM-47) system is:

$$d(m) = 224\left(\frac{L}{100}\right)^{0.4}\left(\frac{I}{10}\right)^{0.2}\left(\frac{\rho}{100}\right)^{0.24}$$

where:

d = depth in metres for which the bottom layer in a two-layer model is detectable, assuming a 3 times resistivity contrast between layers and a noise level of 1 nV/m^2
L = average loop side length (m)
I = current (A)
ρ = resistivity(ohm-m)

Hickin and Best (2013) set the maximum depth of exploration at 130 m for the inversion of the EM-47 before the seismic reflection data were available. This estimate was based on previous experience and an average resistivity value of the upper geological section between 40 and 50 ohm-m, which was obtained from inversions. However, the maximum depth of exploration for the EM-47 system based on the above equation and graph (using L = 100 m, I = 3 A and the same average upper resistivity between 40 and 50 ohm-m) is between 140 and 150 m. We noted the contrast between layers was commonly below 3:1 so d could be lower. Based on these observations, we decided to fix the maximum depth d of exploration for the EM-47 at 150 m for the inversions that were carried out in conjunction with the reflection seismic data.

3.6.2. Inversion of EM data before the reflection seismic survey (Hickin and Best, 2013)

A smooth model inversion with layer thicknesses that increased logarithmically with depth (maximum depth equal to 130 m) was carried out for each sounding to determine the approximate variation of resistivity with depth (option 1 in Hickin and Best, 2013). A 15-layer smooth model was selected because it provided enough detail to estimate significant resistivity variation. These inversions provided a preliminary estimate of the number of layers and their approximate resistivity values required for the multi-layered earth models. The preliminary models estimated from the smooth model were then inverted to produce the best-fit layered-earth model (option 2 in Hickin and Best, 2013). Where possible, boundaries were adjusted to reflect ancillary data or adjacent soundings, without exceeding the standard error achieved by the best-fit model. However, none of the layer depths were fixed for all of these inversions. For further details of this process, example soundings, and the complete interpretation before the reflection seismic data became available see Hickin and Best (2013).

3.6.3. Inversion of EM data in conjunction with reflection seismic and borehole information

Almost all the procedures developed in Hickin and Best (2013) to generate the EM-47 1-D inversions using the Interpex software were also used for this study. The upper EM layer depth was fixed for soundings where seismic reflectors were clearly visible and coherent. About half the soundings had their upper layer fixed. Several soundings had the bedrock depth fixed from the borehole logs (for example Road 269 at the first sounding north of Road 208 (borehole GB 15-2). However, the resistivity, was allowed to vary for all layers. The resistivity and thickness of the layers from the new inversions and the original inversions from Hickin and Best (2013) were nearly identical for most of the soundings where bedrock was shallow (see Table 4 for an example from the 269 Road; Fig. 22). Where bedrock was inferred to be deeper based on seismic interpretations, the inversion from Hickin and Best (2013) and the inversion from our study using seismic constraints were not always as consistent

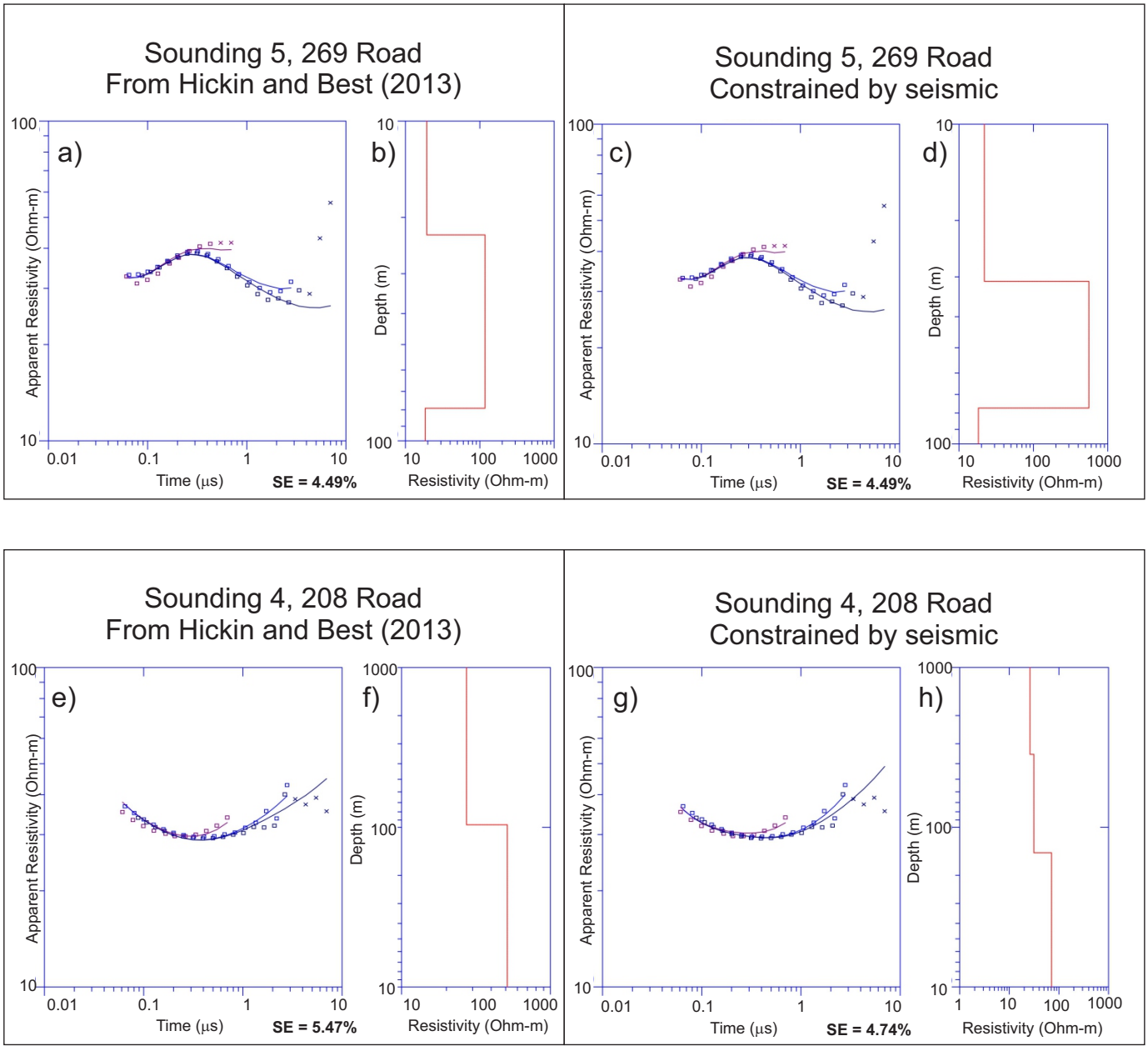

Fig. 22. Four inversions for the examples given in Tables 4 and 5. Each inversion includes the data with the best-fit curves for each frequency (**a, c, e, and g**) and best fit layer model (**b, d, f, and h**); SE = standard errors of fit.

(see Table 5 for an example from the 208 Road, Fig. 22).

Although multi-layer inversions are possible based on the seismic interpretation, it is unlikely that the resolution of the EM-47 data is sufficient to model these complexities. The comments concerning the small resistivity ratios discussed by Hickin and Best (2013) are still valid. The resistivity values of the layers commonly had very small differences, with resistivity ratios less than 3:1, so seismic intervals had to be lumped into single layers for the inversion. Models were kept as simple as possible, subject to the constraints of the boreholes and seismic reflectors. Consequently, the number of layers used in the final inversions varied between two and four (bottom layer goes to infinity with most being 2 or 3).

The maximum depth of an inversion was set to 150 m (see above). However, by limiting the number of layers in the inversion we found very few depths established at the 150 m limit. Where the seismic data (or borehole data) indicated bedrock was deeper than the deepest layer from the inversion, the deepest layer typically had resistivity values that were slightly higher (i.e., 20-30 Ohm-m) than expected from bedrock (10-25 Ohm-m). The deepest layer

Table 4. Comparison of 3-layer inversion from Hickin and Best (2013) and 3-layer inversion using seismic constraint for sounding number 5 (from the south) on 269 Road (see Fig. 19). In this case bedrock is expected to be shallow.

Study	Profile	Sounding	Elevation Range Layer 1 (m)	Resistivity layer 1 (ohm-m)	Elevation Range Layer 2 (m)	Resistivity layer 2 (Ohm-m)	Resistivity layer 3 (Ohm-m)
Hickin & Best (2013)	269 Road	5	707-686	19	686-629	117	18
This study (constrained by seismic data)	269 Road	5	707-678 (fixed at 678)	22	678-631	558	18

Table 5. Comparison of 2-layer inversion from Hickin and Best (2013) and 3-layer inversion using seismic constraint for sounding number 4 (from the west) on 208 Road (see Fig. 19). In this case, bedrock is expected to be deep.

Study	Profile	Sounding	Elevation Range Layer 1 (m)	Resistivity layer 1 (ohm-m)	Elevation Range Layer 2 (m)	Resistivity layer 2 (Ohm-m)	Resistivity layer 3 (Ohm-m)
Hickin & Best (2013)	208[1] Road	4	700-604	27	No value	51	No value
This study (constrained by seismic and/or borehole data)	208 Road[2]	4	700-665 (fixed at 665)	26	665-555	31	71

[1]2-layer model; [2]3-layer model

imaged from these 1-D inversions is therefore expected to be within the Quaternary valley-fill and is probably Unit 7 (e.g., the deepest portion of the paleovalley along the 271 Road; Appendix E).

Adjacent inverted soundings along roads were combined into resistivity cross sections using ArcMap by ESRI. Resistivity values from the 1-D inversion were plotted by distance (x) and elevation (y) with values at 5 m depth increments. Cross sections were contoured using inverse distance weighting interpolation and horizontal anisotropy with a major search radius of 800 m and a minor search radius of 10 m (conducted in Geostatistical Analyst). This interpolation method was selected because it is an exact interpolator (honours data points) and the anisotropic search radius accounts for higher vertical data density than horizontal data density. All cross sections are provided in Appendix D.

4. Discussion

In general, the seismic and EM data are complementary, helping to interpret paleovalley geometry and the valley-fill sequences. The reflectors constrain unit boundaries, and interval velocities corroborate resistivity data interpretations, particularly in the upper 100 m. Unfortunately, we designed our survey anticipating depths to bedrock of less than about 100 m and our data indicate that the bedrock surface in the deepest part of the paleovalley may be as deep as 250-350 m. The resultant loss of resolution from a design that is less than optimal for depths > 100 m leads to ambiguities in the depth to bedrock and the valley-fill architecture in the deep portions. Nonetheless, establishing the exceptional and unexpected depths of the Groundbirch paleovalley is significant for documenting the configuration of the regional paleovalley network.

The EM data can be interpreted to represent generalized lithologic domains reflecting clay content and air- and water-filled pore space. High resistivity is inferred to represent coarse-grained domains (sand and gravel) and low resistivity, fine-grained domains. The resistivity contrasts between units in the valley fill and between the valley-fill and bedrock are generally small (commonly only a factor of 3 or less). Resistivity values between units commonly overlap, making the interpretation of the EM data problematic. The seismic data better resolve boundaries of contrasting acoustic impedance and provides the framework for the valley fill.

The data from the 269 Road are useful for illustrating the integrated seismic and EM data. Combining the EM and seismic data with drilling information (Fig. 23), six generalized domains can be recognized and correlated to the regional stratigraphy. The lowest domain, D1, is interpreted to be bedrock. D2 is >200 m thick and interpreted to be Unit 7, advance phase glaciolacustrine sediments. D3 is 10-15 m thick and is interpreted to be a coarse-grained portion of Unit 7, Unit 8 (alluvial fan) or a gravel-rich portion of Unit 9 (glacial complex). D4 is 10-25 m thick and, although mainly equivalent to Unit 9, may include a combination of units 8 and 9. D5 is discontinuous and represents the coarse-grained (sand or gravel) ice-contact glaciolacustrine sediments of Unit 10. D6 is interpreted to be the fine-grained component of Unit 10, the retreat phase glaciolacustrine deposit.

D1 is below the reflector interpreted as the bedrock-Quaternary sediment contact. Resistivity values in D1 are typically between 10-20 Ohm-m (ranging up to 28 Ohm-m). Locally (e.g., north end of 271 Road), slightly higher values (~30 Ohm-m) were recorded, which may represent slightly coarser-grained bedrock (siltstone or fine-grained sandstone).

Where the paleovalley is deepest, the bedrock reflector is not well represented by the seismic data and is commonly weak or not coherent. This may be because the reflector is too deep to be detected or the paleovalley walls are too steep to generate a coherent reflection (diffraction/scattering). Alternatively, an irregular contact can scatter seismic energy resulting in an incoherent reflection. Borehole GB 15-1 shows that the bedrock-sediment contact is a zone of breccia, with sediment injections penetrating subjacent bedrock over several metres. Such a contact could produce an irregular surface that prohibits a coherent reflection. It is also possible that the contrast between the acoustic impedance of clay-rich diamict and clay-rich bedrock is too weak to generate a coherent reflection. For the deeper portions of the paleovalley, we lack direct borehole evidence of where the bedrock surface is positioned. Albeit tentative, we must therefore rely on our interpretation that the seismic reflector records the bedrock-cover contact. Consistent with this interpretation is the observation that where the drilling failed to intersect bedrock to a depth of at least 145 m (e.g., GB 15-2 and GB 15-5), the seismic data predicted a thick paleovalley fill, with the reflector positioned at significantly greater depths. Further drilling is required to test our interpretation of the reflector.

In some places the seismic interpretation and the EM data conflict. For example, interpretation of the seismic data implies thick diamict below the ridge on the north ends of 271, 269 and 267 roads (south of Highway 97). The interpreted EM data show bedrock nearly to surface on this ridge. These conflicting interpretations are common (cf. Sapia et al., 2015) and can only be resolved by drilling.

In the deepest portions of the paleovalley, D2 occurs above bedrock. D2 is a semi-transparent seismic zone with velocities consistent with fine sand and silt. Resistivity values, typically about 40 Ohm-m (range, 20-250 Ohm-m) are compatible with this interpretation, but also indicate coarser-grained regions in this zone (i.e. where values are >100 Ohm-m). Lithologies encountered in boreholes GB 15-2 and GB 15-5 include clay, silt and sand from Unit 7.

Domains D3, D4, and D5 are distinguished mainly by the seismic facies because the EM data cannot resolve stratigraphic details. Differentiating the domains helps understand how the geophysical domains relate to the stratigraphic units. The boundary between D2 and D3 is marked by a strong, relatively continuous, undulating P-wave reflection. D3 occurs as a 10 m-thick zone in the S-wave data, with velocities that suggest gravel. Resistivity is typically about 80 Ohm-m, but shows a large range (10 - >250 Ohm-m), which reflects the limited resolution of the method. Although this domain can be separated from D3 and D4, D3 is genetically linked to the transition from glaciolacustrine (Unit 7) to subglacial deposits (Unit 9) and may include deposits of both, as well as Unit 8 mass wasting deposits. For modeling, D3 is generally included in Unit 7. D4 is a high-velocity seismic zone with resistivity values that range from 20 to >350 Ohm-m. Boreholes GB 15-1 and GB 15-4 record 10-20 m of till, but thick till is absent in boreholes GB 15-2 and GB 15-5. The diamict in GB 15-3 is interstratified with silt and sand. D4 is, therefore, interpreted to consist of interbedded units of silt, sand, gravel, and till (Unit 9).

D5 is a discontinuous semi-transparent seismic zone,

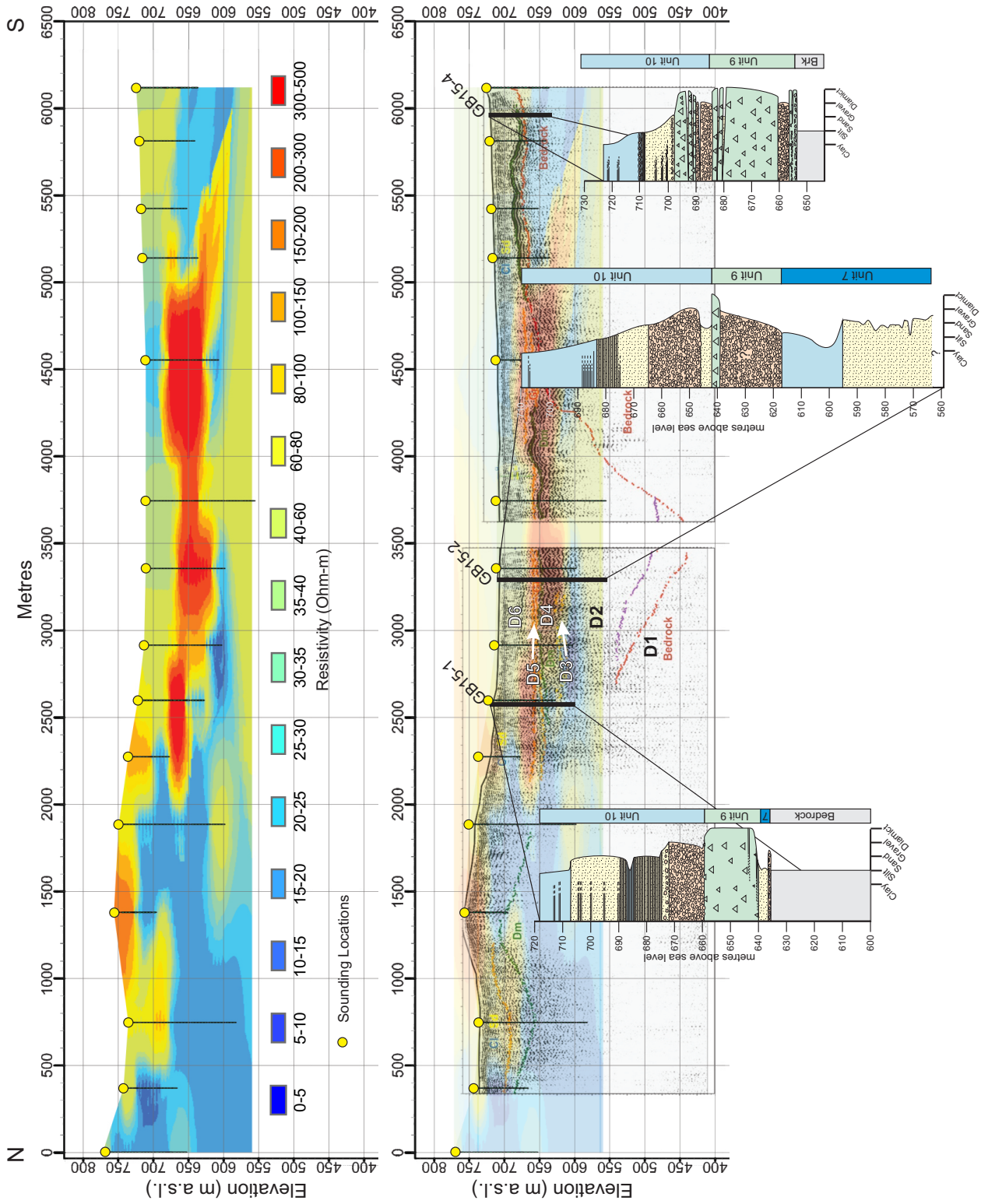

Fig. 23. Geophysical data and lithology logs from the 269 Road. **a)** EM profile, where warm colours represent higher resistivity (likely coarser-grained lithologies) and cool colours represent low resistivity (fine-grained lithologies). **b)** EM profile overlain onto the seismic data with lithology logs from boreholes plotted (heavy black vertical bars are the locations of the boreholes).

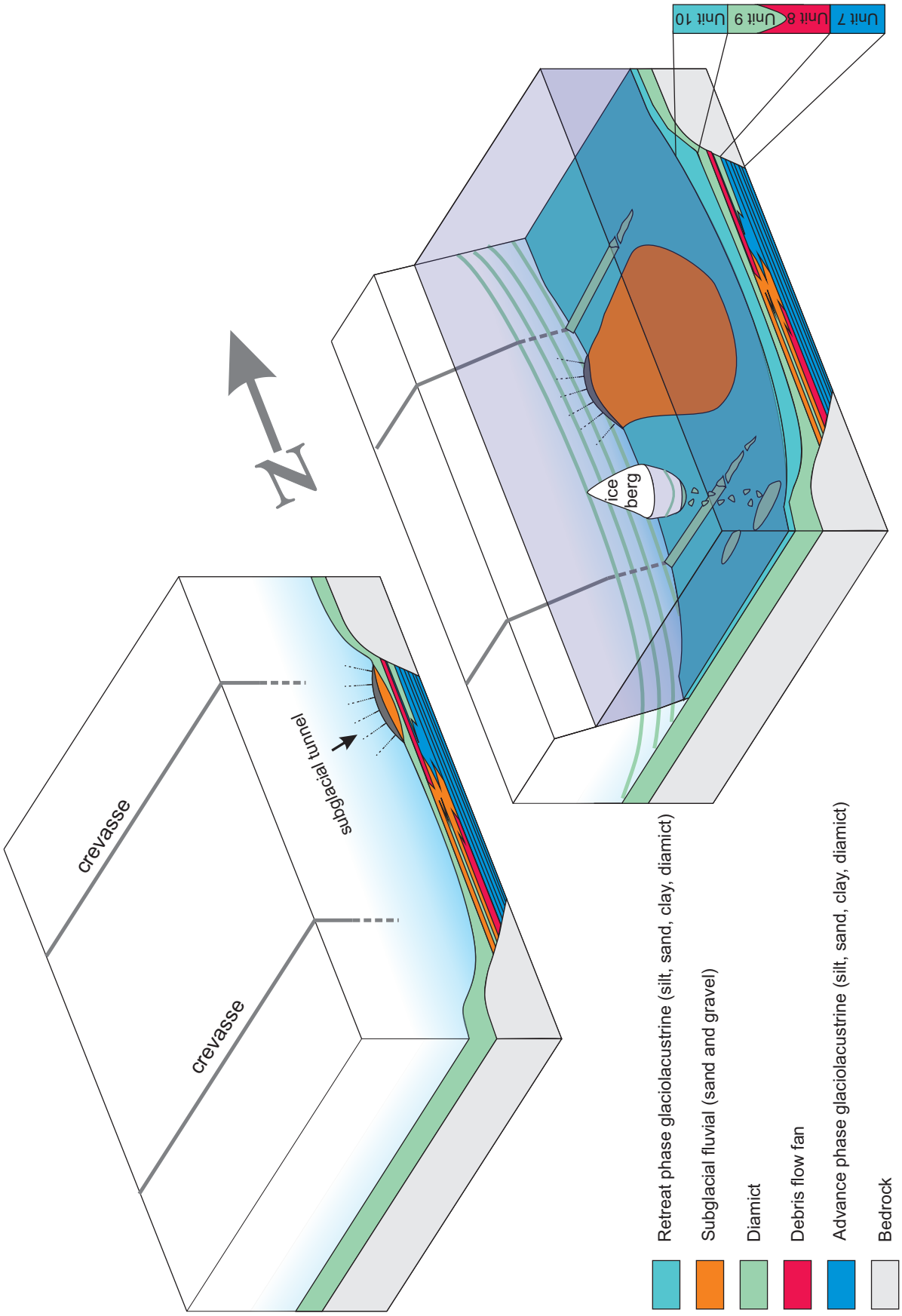

Fig. 24. Block model showing depositional settings in the Groundbirch paleovalley at the ice margin during ice sheet retreat.

commonly in depressions defined by the strong S-wave reflections at the top of D4. Resistivity values are highly variable and range from 20 to >350 Ohm-m. All the boreholes intersect coarse-grained sediments (sand or gravel) immediately above the Unit 9 deposits and interpreted to be part of Unit 10. Therefore, D5 is interpreted to represent coarse sedimentation at the transition between an ice-contact setting and a retreat phase glacial lake setting.

Sedimentation of units in domains D3-D5 was probably during: 1) ice advance into glacial Lake Mathews; 2) full glacial conditions (subglacial); and 3) ice retreat from glacial Lake Peace (Fig. 24). Till is thickest at the margins of the paleovalley where bedrock is interpreted to be close to surface. Sediments are more variable above the deepest portion of the paleovalleys where the underlying advance phase glaciolacustrine sediments are thickest. Glaciolacustrine sediments were likely water saturated and highly deformable, perhaps limiting the deposition of a thick till blanket. The other interstratified sediments likely reflect a variety of depositional processes at the ice margin during both advance and retreat (e.g., subglacial fluvial discharge, suspension settling, rainout of ice-rafted debris). The uppermost domain, D6 consists of a distinct high-frequency seismic facies. Its base is marked by either a strong and continuous reflector or is inferred where the semi-transparent transparent seismic zone of D5 is defined. Resistivity values from this horizon range from 20 to >300 Ohm-m and are laterally variable. Boreholes and surface exposures indicate that D6 consists of silt, sand and clay, which we interpret as having been deposited in glacial Lake Peace (Unit 10).

Collectively, the data across multiple data acquisition lines provide a consistent geological framework that represents the geometry and valley fill of the Groundbirch paleovalley (Figs. 25 and 26). The main valley trends east-west and plunges to the west. It is 3000-4000 m wide at its maximum. Although the base of the paleovalley is not well imaged, seismic data from the 269 Road may indicate that the base of the valley narrows to a V-shape. To the north, a bedrock ridge separates the Groundbirch paleovalley from a tributary valley under Highway 97. These valleys join to the west.

Coarse-grained sediments, which hold the highest potential for aquifers, should display the highest resistivity values. The highest resistivity values in the survey are along the Groundbirch paleovalley between 675 and 625 m above sea level (asl) which, consistent with the geologic data, correspond to D3 and D5 at the upper and lower contact of Unit 9 (Fig. 27). Subglacial discharge of sand and gravel probably preceded and followed the advancing and retreating ice margin. Consequently a discontinuous apron of sand and gravel was likely deposited immediately below till, within the deforming layer, and immediately above till. All boreholes show significant saturated sand and gravel above and below diamict and these lithologies are considered excellent aquifer targets. The clay-rich tills that separate these potential sand- and gravel- aquifers might constitute aquitards. Because these tills are locally absent, the aquifers would likely connect hydraulically.

Moderate resistivity values (30-100 Ohm-m) are from sandy intervals, which also hold aquifer potential. Resistivity values in this range are common in the advance (Unit 7) and retreat phase (Unit 10) glaciolacustrine deposits (see geologic maps, right side of Fig. 27). In the advance phase glaciolacustrine unit (Unit 7), moderate values consistently occur in the deepest sections of the Groundbirch paleovalley. Both boreholes GB 15-2 and GB 15-5 intersected a thick section of water-saturated fine- to medium- sand at the base of the cored section (see Figs. 6 and 11). The retreat phase glaciolacustrine deposit (Unit 10) typically contains gravel or coarse sand at the base of the succession and fines upwards (Hickin, 2013). These coarse-grained units in Unit 10 have high potential as aquifers. In addition, moderate to high resistivity values along the upper margins of the paleovalley could also indicate potential aquifers.

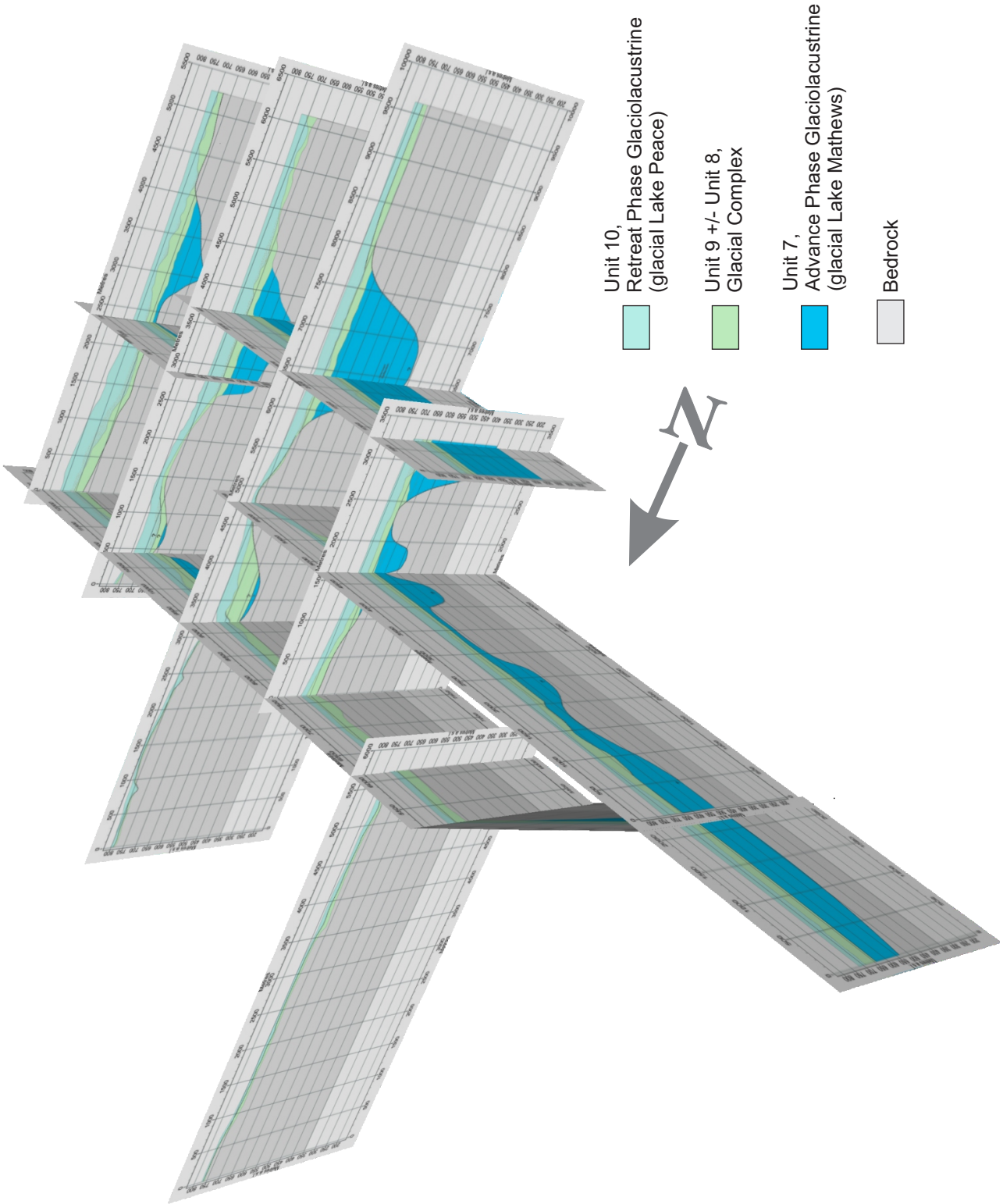

Fig. 25. Fence diagram showing Groundbirch Paleovalley (view to the east).

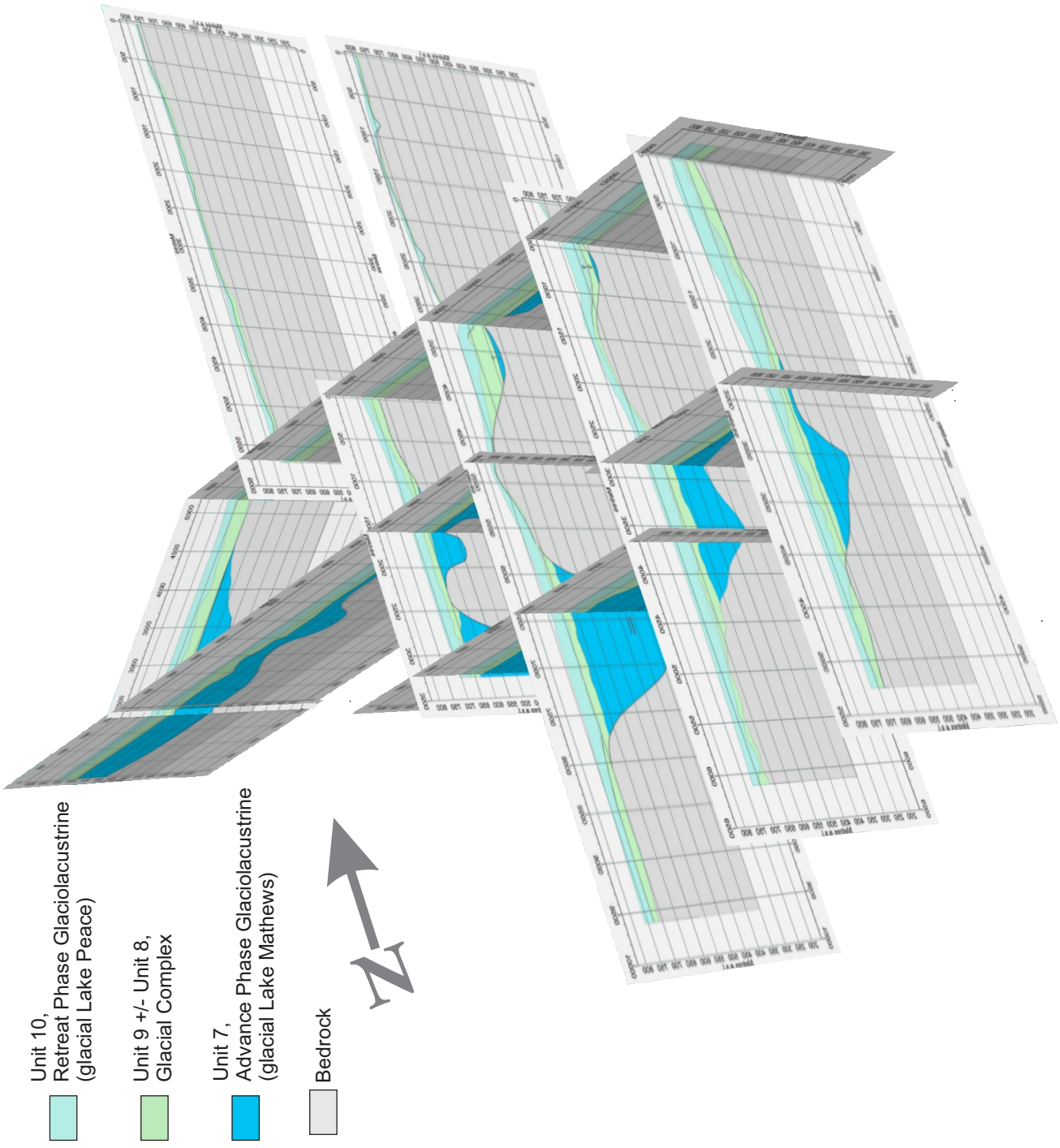

Fig. 26. Fence diagram showing Groundbirch paleovalley (view to the west).

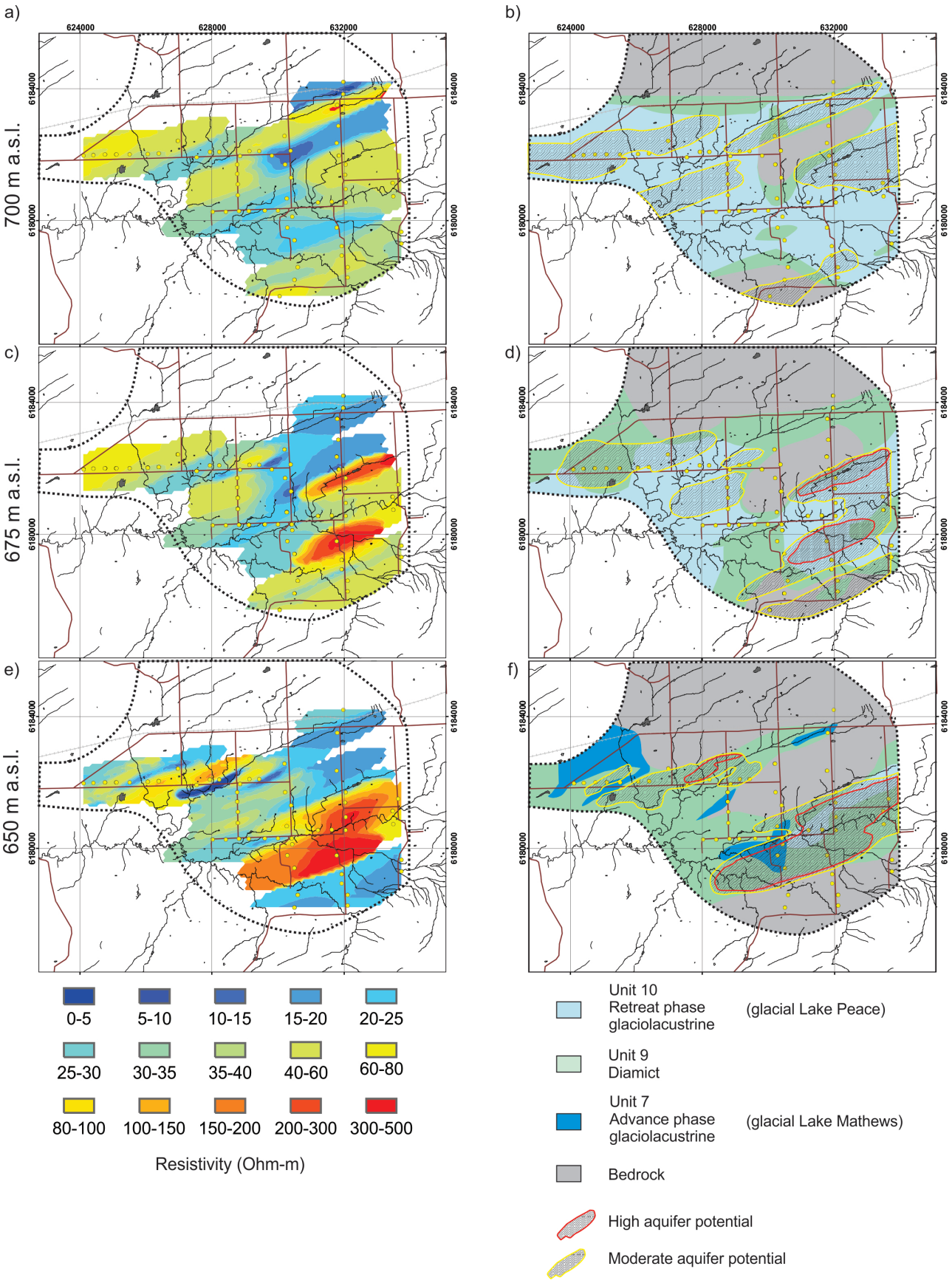

Fig. 27. Elevation slices showing resistivity (**a, c, e, g, i, and k**) and stratigraphy and aquifer potential (**b, d, f, h, j, k, and l**).

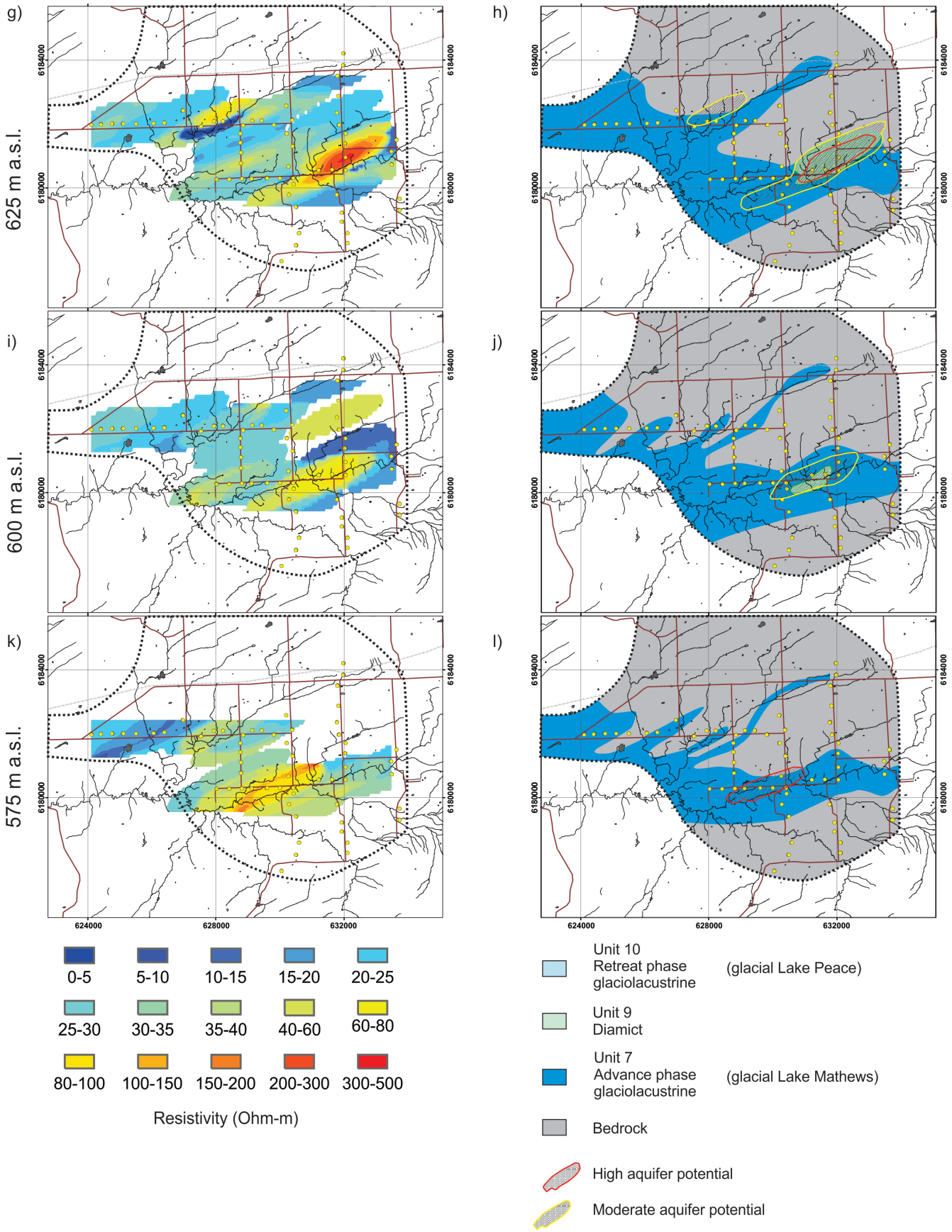

Fig. 27. continued.

5. Summary

This study was designed to refine the geometry of the Groundbirch paleovalley and establish a stratigraphic framework for the valley fill, thereby improve the understanding of groundwater aquifer potential in the region.

1). The combination of ground-based electromagnetic (EM) and shallow seismic geophysical surveys coupled with direct observation of subsurface lithology (through sediment coring) has better defined the geometry and valley-fill stratigraphy of the Groundbirch paleovalley. Limited resistivity contrast within the valley-fill units and between the valley fill and bedrock makes interpretation of the EM inversions challenging. These drawbacks are partially overcome through the seismic data. Where the EM data depicts mainly grain-size and pore space, the seismic data reveals unit geometry. The complementary methods were most effective in the upper 75 m of the survey area. The large loop EM method deployed in this survey is effective to a maximum depth of 150 m. Unfortunately, the seismic survey design was not optimized for the unexpected depth of the paleovalley, so imaging the bedrock-sediment interface in the deepest portions of the paleovalley was not achieved and the true depth and configuration of the valley bottom remains ambiguous.

2). The interpretation of the combined data suggests that the Groundbirch paleovalley probably trends generally east-west, and plunges to the west. The valley is approximately 3-4 km wide at its top and, where imaging was successful (i.e. 269 Road), it narrows to a V-shaped bottom. Although ambiguous, taken at face value the seismic data indicate that the base of the paleovalley may be more than 350 m below surface. This is an extraordinary and unexpected depth, which can be tested by drilling to bedrock.

3). The stratigraphy of the valley fill is consistent with the regional stratigraphy proposed by Hickin, (2013). The fill succession that can be resolved by the seismic and EM data correlates with the advance phase glaciolacustrine sediments (Unit 7, glacial Lake Mathews), ice-contact glacial sediments (mainly Unit 9 and possibly Unit 8), and retreat phase glaciolacustrine deposits (Unit 10, glacial Lake Peace).

4). Gravels and sands deposited at the ice margin during glacier advance and retreat have high potential to host significant aquifers. These sediments occur immediately below and above clay-rich diamicts of Unit 9, which could serve as aquitards. However, because the diamicts are laterally discontinuous over the thickest valley fill, these aquifers are probably hydraulically connected.

Acknowledgments

We thank all those who collaborated with us as part of the Northeast British Columbia Aquifer Characterization Project. We are particularly grateful to Chelton van Geloven for his tireless efforts and outstanding coordination, which were integral to the success of this study and the entire project. Dr. Dave Wilford championed the project and provided oversight. Funding and in-kind support were by BC Ministry of Forests, Lands, and Natural Resource Operation, BC Ministry of Energy and Mines, Geological Survey of Canada, Geoscience BC, and Shell Canada Limited. Dr. Victor Levson (Quaternary Geoscience Inc.) and Dr. Brent Ward (Simon Fraser University) logged the core. Drilling was by Westech Drilling Corp. and Mud Bay Drilling Ltd., and geophysical core logging was by Weatherford International plc. Insightful comments and through reviews by Dr. Victor Levson and Dr. Lawrence Aspler improved the paper.

References cited

Aber, J.S. and Ber, A., 2007. Glaciotectonism. Elsevier, 246 pp.

Ahmad, J., Schmitt, D.R., Rokosh, C.D., and Pawlowicz, J.G., 2009. High-resoluition seismic and resistivity profiling of a buried Quaternary subglacial valley: Northern Alberta, Canada. Geological Society of America Bulletin, 121, 1570-1583.

Ashley, G.M., Southard, J.B., and Boothroyd, J.C., 1982. Deposition of climbing-ripple beds: a flume simulation. Sedimentology, 29, 67-79.

Callan, D.M., 1970. An investigation of a buried channel deposit in the Groundbirch area of northeastern British Columbia. Report No. 3 of 1969 Peace River Rotary Drilling Programme, British Columbia Ministry of Environment, Groundwater Division.

Cohen K.M., and Gibbard, P., 2011. Global chronostratigraphical correlation table for the last 2.7 million years. Subcommission on Quaternary Stratigraphy (International Commission on Stratigraphy), Cambridge, England.

Constable, S.C., Parker, R.L., and Constable,C.G., 1987. Occam's inversion: A practical algorithm for generating smooth models from electromagnetic sounding data.

Geophysics, 52, 289-399.

Cowen, A., 1998. BC Peace Region Groundwater Initiative Interim Report 1998. Prairie Farm Rehabilitation Administration.

Dreimanis, A., 1988. Tills: Their genetic terminology and classification. In Goldthwait, R.P. and Matsch, C.L. (eds), Genetic classification of Glacigenic deposits, A.A. Balkema, Rotterdam, 17-68.

Eyles, C.H. and Eyles, N., 2010. Glacial Deposits. In James, N.P. and Dalrymple, R.W. (eds.): Facies Models 4. Geological Association of Canada, St. John's, 73-104

Freeze, R.A., and Cherry, J.A., 1979. Groundwater. Prentice-Hall, Englewood Cliffs, NJ, USA.

Geonics, 2011, Protem 47D operating manual for 20/30 gate model. Geonics Limited, Mississauga, Ontario

Hartman, G.M.D. and Clague, J.J., 2008. Quaternary stratigraphy and glacial history of the Peace River valley, northeast British Columbia. Canadian Journal of Earth Sciences, 45, 549-564.

Hickin, A.S., 2011. Preliminary bedrock topography and drift thickness of the Montney Play area. British Columbia Ministry of Energy and Mines, Energy Open File 2011-1 and Geoscience BC, Report 2011-07, 2 maps, 1:500 000 scale.

Hickin, A.S., 2013. Late Quaternary to Holocene geology, geomorphology, and glacial history of Dawson Creek and surrounding area, Northeast British Columbia, Canada. PhD Thesis, University of Victoria, Victoria, B.C.

Hickin, A.S. and Best, M.E., 2012. Stratigraphy and proposed geophysical survey of the Groundbirch paleovalley: Contribution to the collaborative northeast British Columbia aquifer project. In Geoscience Reports 2012, British Columbia Ministry of Energy and Mines, 91-103.

Hickin, A.S. and Best, M.E., 2013. Mapping the geometry and lithostratigraphy of a paleovalley with a time-domain electromagnetic technique in an area with small resistivity contrasts, Groundbirch, British Columbia, Canada. Journal of Environmental and Engineering Geophysics, 18, 119-135.

Hickin, A.S., Lian, O.B., and Levson. V.M., in press. Coalescence of late Wisconsinan Cordilleran and Laurentide ice sheets east of the Rocky Mountain Foothills in the Dawson Creek region, Northeast British Columbia, Canada. Quaternary Research, DOI: 10.1016/j.yqres.2016.02.005.

Hickin, A.S. Kerr, B., Barchyn, T.E., and Paulen, R.C., 2009. Using ground-penetrating radar and capacitively coupled resistivity to investigate 3-D fluvial architecture and grain-size distribution of a gravel floodplain in northeast British Columbia, Canada. Journal of Sedimentary Research, 70, 457-477.

Hickin, A.S., Kerr, B., Turner, D.G., and Barchyn, T.E., 2008. Mapping Quaternary paleovalleys and drift thickness using petrophysical logs, northeast British Columbia, Fontas map sheet, NTS 94I. Canadian Journal of Earth Sciences, 45, 577-591.

Hickin, A.S., Lian, O.B., Levson, V.M. and Cui, Y., 2015. Pattern and chronology of glacial Lake Peace shorelines and implications for isostacy and ice sheet configuration in northeastern British Columbia, Canada. Boreas, 44, 288-304.

Hooke, R. LeB., 1967. Processes on arid-region alluvial fans. Journal of Geology, 75, 438-460.

Interpex, 2006, IX1D.v3 tutorials. Interpex Limited, Golden, Colorado.

Lowe, D.R., 1979. Sediment grain flows: Their classification and some problems of application to natural flows and deposits. In Doyal, L. and Pilkey, O.H. (eds) Geology of continental slopes. SEPM Special Publication 27, 75-82.

Lowen, D., 2011. Aquifer classification mapping in the Peace River Region for the Montney water project. Unpublished, Lowen Hydrogeology Consulting Ltd. File no. 1026.

Mathews, W.H., 1955, Ground-water possibilities of the Peace River block, British Columbia. British Columbia Ministry of Energy and Mines, Groundwater Paper 3.

Mathews, W.H., 1978, Quaternary stratigraphy and geomorphology of the Charlie Lake (94A) map-area, British Columbia. Geological Survey of Canada, Paper 76-20.

Mathews, W.H. 1980. Retreat of the last ice sheets in northeastern British Columbia and adjacent Alberta. Geological Survey of Canada, Bulletin 331.

McMechan, M.E., 1994, Geology and structure cross-section, Dawson Creek, British Columbia. Geological Survey of Canada, Map 1858A.

Miall, A.D., 2006.The Geology of Fluvial Deposits; Sedimentary Facies, Basin Analysis, and Petroleum Geology, 4th Printing. Springer, New York.

McNeill, J.D., 1994, Principles and applications of time-domain electromagnetic techniques for resistivity sounding. Geonics Limited, Technical Note TN27.

Occhietti, S. 1973. Les structure et déformations engendrées par les glacier – Essai de mise au point. Revue Géographique de Montréal, 27, 365-380

Oldenborger G.A., Pugin A.J.-M. and Pullan S.E., 2013. Airborne time-domain electromagnetics, electrical resistivity and seismic reflection for regional three-dimensional mapping and characterization of the Spiritwood Valley Aquifer, Manitoba, Canada. Near Surface Geophysics, 11, 63-74.

Pawlowicz, J.G., Hickin, A.S., Nicoll, T.J., Fenton, M.M., Paulen, R.C., Plouffe, A., and Smith, I.R., 2005, Bedrock topography of the Zama Lake Area, Alberta (NTS 84L). Alberta Energy and Utilities Board, Alberta Geological Survey, Map 328.

Pawlowicz, J.G., Nicoll, T.J., and Sciarra, J.N., 2007, Bedrock topography of Bistcho Lake area, Alberta (NTS 84M). Alberta Energy and Utilities Board, Alberta Geological Survey, Map 416.

Pugin, A. J.-M, Pullan S.E. and Sharpe, D.R., 1999. Seismic facies and regional architecture of the Oak Ridges Moraine area, southern Ontario. Canadian Journal of Earth Sciences, 36, 409-432.

Pugin, A. J.-M, Pullan S.E. and Hunter, J.A., 2009. Multicomponent high-resolution seismic reflection profiling. The Leading Edge, 28, 1248-1261.

Pugin, A. J.-M, Oldenborger, G.A., Cummings, D.I., Russell, H.A.J., and Sharpe, D.R., 2014. Architecture of buried valleys in glaciated Canadian Prairie regions based on high resolution geophysical data. Quaternary Science Reviews, 86, 13-23.

Reimchen, T.H.F., and Rutter, N.W., 1972. Quaternary geology, Dawson Creek, British Columbia: Geological Survey and Canada, Report of Activities, Part A, Paper 72-1, 176-177.

Reitz, J.R., and Milford, F.J., 1962. Foundations of electromagnetic theory. Addison-Wesley Publishing Company, Reading, MA., USA.

Sapia, V., Oldenborger, G.A., Jørgensen, F., Pugin, A. J.-M., Marchetti, M., Viezzoli, A., 2015, 3D modeling of buried valley geology using airborne electromagnetic data Interpretation. Interpretation, 3, SAC9-SAC22.

Smith, G.A. and Lowe, D.R., 1991. Lahars: volcano – hydrologic events and deposition in the debris flow-hyperconcentrated flow continuum. In Fisher, R.V., Smith, G.A. (eds), Sedimentation in Volcanic Settings. SEPM Special Publication, 45, 60-70.

Spies, B.R., 1983. Limitations and survey design parameters for transient electromagnetic surveys. SEG Technical Program, Expanded Abstracts, 638-642

Spies, B.R. and Eggers, D.E., 1986. The use and misuse of apparent resistivity in electromagnetic methods. Geophysics, 51, 1462-1471.

Stott, D.F., 1961. Summary account of the Cretaceous and equivalent rocks, Rocky Mountain Foothills, Alberta. Geological Survey of Canada, Paper 61-2, 34p.

Van Dam, R.L., 2012. Landform characterization using geophysics-Recent advances, applications, and emerging tools. Geomorphology, 137, 57-73.

Wilford, D., Hickin, A.S., Chapman, A., Kelly, J., Janicki, E.P., Kerr, B., van Geloven, C., Dessouki, T., Henry, K., Heslop, K., Kirste, D., McCarville, M., Ronneseth, K., Sakals, M., Wei, M., 2012. Collaborative interagency water projects in Britsh Columbia: Introduction to the northeast British Columbia aquifer project and streamflow modelling decision support tool. In Geoscience Reports 2012, British Columbia Ministry of Energy and Mines, 79-89.

British Columbia Geological Survey
Ministry of Energy and Mines
www.em.gov.bc.ca/geology